



This is a repository copy of *Energy metrics to evaluate the energy use and performance of water main assets*.

White Rose Research Online URL for this paper:

<https://eprints.whiterose.ac.uk/120016/>

Version: Accepted Version

---

**Article:**

Hashemi, S., Filion, Y.R. and Speight, V. orcid.org/0000-0001-7780-7863 (2018) Energy metrics to evaluate the energy use and performance of water main assets. *Journal of Water Resources Planning and Management*, 144 (2). 04017094. ISSN 0733-9496

[https://doi.org/10.1061/\(ASCE\)WR.1943-5452.0000857](https://doi.org/10.1061/(ASCE)WR.1943-5452.0000857)

---

This material may be downloaded for personal use only. Any other use requires prior permission of the American Society of Civil Engineers. This material may be found at [https://doi.org/10.1061/\(ASCE\)WR.1943-5452.0000857](https://doi.org/10.1061/(ASCE)WR.1943-5452.0000857)

**Reuse**

Items deposited in White Rose Research Online are protected by copyright, with all rights reserved unless indicated otherwise. They may be downloaded and/or printed for private study, or other acts as permitted by national copyright laws. The publisher or other rights holders may allow further reproduction and re-use of the full text version. This is indicated by the licence information on the White Rose Research Online record for the item.

**Takedown**

If you consider content in White Rose Research Online to be in breach of UK law, please notify us by emailing [eprints@whiterose.ac.uk](mailto:eprints@whiterose.ac.uk) including the URL of the record and the reason for the withdrawal request.



[eprints@whiterose.ac.uk](mailto:eprints@whiterose.ac.uk)  
<https://eprints.whiterose.ac.uk/>

## Energy Metrics to Evaluate the Energy Use and Performance of Water Main Assets

Saeed Hashemi<sup>1</sup>, Yves R. Filion<sup>2</sup>, Vanessa L. Speight<sup>3</sup>

---

**Abstract:** Managing aging infrastructure has become one of the greatest challenges for water utilities, particularly when faced with selecting the most critical pipes for rehabilitation from amongst the thousands of candidates. The aim of this paper is to present a set of novel yet practical energy metrics that quantify energy interactions at the spatial resolution of individual water mains to help utilities identify pipes for rehabilitation. The metrics are demonstrated using a benchmark system and two large, complex systems. The results show that the majority of pipes have a good energy performance but that an important minority of outlier pipes have a low energy efficiency and high energy losses due to friction and leakage. Pumping and tank operations tend to drive energy efficiency and energy losses in pipes close to water sources while diurnal variation in demand drives energy performance of mains located far away from water sources. The new metrics of energy lost to friction and energy lost to leakage can provide information on energy performance in a pipe than is complementary to the traditional measures of unit headloss and leakage flow.

*Keywords:* Energy efficiency, energy metrics, friction loss, leakage loss, pipe rehabilitation, water distribution systems.

---

<sup>1</sup> Saeed Hashemi, Graduate Student, Queen's University, Kingston, Ontario, Canada, K7L 3N6 (e-mail: [s.hashemi@queensu.ca](mailto:s.hashemi@queensu.ca)).

<sup>2</sup> Yves R. Filion, Associate Professor, Queen's University, Kingston, Ontario, Canada, K7L 3N6 (e-mail: [yves.filion@civil.queensu.ca](mailto:yves.filion@civil.queensu.ca)).

<sup>3</sup> Vanessa Speight, Senior Research Fellow, University of Sheffield, Sheffield, UK, S1 3JD, (e-mail: [v.speight@sheffield.ac.uk](mailto:v.speight@sheffield.ac.uk)).

22 **Introduction**

23 Water distribution systems play host to a multitude of energy interactions on an hourly and  
24 daily basis. Pumps and reservoirs supply mechanical energy to the system, while water demand,  
25 pipe leaks, and frictional headloss provide output pathways for energy to leave the system, either  
26 in the form of work or heat. As water main assets in a system age and deteriorate, they become  
27 less energy efficient, with more energy leaving the system via unwanted pipe leaks and through  
28 frictional headloss (Fontana et al., 2012; Kleiner and Rajani, 2001). The challenge in managing  
29 a large, aging water distribution system is to prioritize interventions so that investment returns  
30 the largest gain in system performance (Alvisi and Franchini, 2009 and 2006, Dandy and  
31 Engelhardt, 2001).

32 Energy has long been used as a key concept to understand the performance of engineering  
33 systems (Pelli and Hitz 2000; Lambert et al., 1999). Energy use as a modeling concept is  
34 germane to understanding the energy performance of water main assets in distribution systems  
35 because power and energy in water distribution systems depend on pressure and flow – two  
36 quantities that are monitored continuously by water utilities (Dziedzic and Karney, 2015;  
37 AWWA, 2009; Boulos et al., 2006). While most municipalities extensively monitor their  
38 systems, few have a firm understanding of the energy efficiency of their systems. Even fewer  
39 municipalities have the capability to use pressure and flow data to understand the impact of  
40 infrastructure upgrades and operational changes on the energy efficiency of their systems  
41 (Engelhardt et al., 2000; Roshani and Fillion, 2013; Hashemi et al., 2012).

42 To date, previous research has been focused on characterizing the system-wide energy  
43 dynamics in distribution systems. Colombo and Karney (2002) showed that diurnal  
44 demand/pressures can affect the manner in which fissures and cracks in pipes conduct leakage.

45 Results demonstrated that the more distant the leakage sources are from the water sources, the  
46 higher is the energy lost from leakage and friction. While, the presence of storage was shown to  
47 have a negligible effect on leakage energy, the location of the tanks did influence the leakage  
48 level and pumping energy (Colombo and Karney 2005). The research underscored the important  
49 role of water mains, and their proximity to pumps and tanks, on the energy balance of a system.

50 Energy metrics developed thus far have focused on the system-wide energy performance of  
51 systems. Pelli and Hitz (2000) developed energy indicators to relate system-wide energy  
52 efficiency to pump efficiency and reservoir location, without considering leakage impacts.  
53 Cabrera et al. (2010) presented a set of metrics to characterize the system-wide energy  
54 performance that includes losses to friction, leakage, and overpressure. These energy metrics  
55 provide a useful set of tools to help water utility managers better understand how far their  
56 systems are from an ideal energy-efficient state but fall short of being able to identify individual  
57 pipes that are problematic. Building upon their earlier work, Cabrera et al. (2014b) presented  
58 additional metrics to assess the energy efficiency of a pressurized system and procedures to  
59 prioritize interventions on a system-wide basis. Dziejczak and Karney (2014) examined the  
60 energy dynamics of groups of pipes and pumps in the Toronto distribution system. While these  
61 researchers also solved the energy balance to examine the frictional losses in individual pipes of  
62 the Toronto system, they did not examine the efficiency, leakage, and other energy  
63 characteristics of these pipes. The current paper extends this research direction by considering  
64 energy transformations that take place in the individual pipes of a distribution system.

65 The aim of this paper is to present a set of novel energy metrics that quantify energy  
66 interactions in a distribution system at the spatial resolution of individual water mains. These  
67 pipe-level metrics can be applied to: 1) characterize the energy performance in water mains in an

68 unimproved state to establish a benchmark prior to any rehabilitation work; 2) plan infrastructure  
69 upgrades and operational changes in areas that exhibit a low energy efficiency alongside  
70 information on cost, water quality, and pipe break history, and; 3) characterize the impact of  
71 infrastructure upgrades and operational improvements on the energy performance of water mains  
72 in a system. In this paper, the new pipe-level metrics are applied to a large *ensemble* of water  
73 mains across three distribution systems to examine how system operation and system  
74 improvements impinge on the spatial and temporal patterns of energy performance in drinking  
75 water mains.

## 76 **Energy Use in a Pipe**

77 To develop a set of energy metrics, it is instructive to consider the hydraulic grade line with  
78 energy inputs and outputs in a single pipe as indicated in Figure 1. Here, the pipe conveys a flow  
79  $Q$  ( $\text{m}^3/\text{s}$ ) at an upstream pressure head  $H_s$  (m). The pipe delivers a pressure head  $H_d$  (m) to a  
80 downstream user that imposes a demand  $Q_d$  ( $\text{m}^3/\text{s}$ ) in the pipe. Users downstream of a pipe  
81 impose a demand  $Q_d$  ( $\text{m}^3/\text{s}$ ) that exceeds the minimum needed water use  $Q_{\min}$  ( $\text{m}^3/\text{s}$ ), which  
82 represents the most efficient use of water by the user given best-available water technologies  
83 (Vickers 2001). There are a number of reasons for this inefficient water use including household  
84 leaks, inefficiencies in appliances, theft of water (AWWA 2009), water waste through inefficient  
85 industrial processes (Morales et al. 2011; Friedman et al. 2011), user perception of appropriate  
86 water use (Hoekstra and Chapagain 2007), and unnecessary lawn and garden watering (Askew  
87 and McGuirk 2004). For the sake of generality, the pipe can have a leak that produces a leakage  
88 flow rate of  $Q_l$  ( $\text{m}^3/\text{s}$ ). The pipe also conveys an additional flow  $Q_{\text{ds}}=Q-Q_d-Q_l$  ( $\text{m}^3/\text{s}$ ) to users  
89 further downstream of the pipe. The upstream pressure head  $H_s$  (m) supplied to the pipe is  
90 greater than the minimum required pressure head  $H_{\min}$  (m) needed to provide an acceptable

91 service to the downstream user. The difference between supplied head  $H_s$  (m) and pressure head  
 92 delivered  $H_d$  (m) is made up of local losses  $H_{local}$  (m) (e.g., valves, in-line turbines, blockages)  
 93 and the combined frictional head loss due to demand  $Q_d$  (m<sup>3</sup>/s), leakage  $Q_l$  (m<sup>3</sup>/s), and the  
 94 additional flow  $Q_{ds}$  (m<sup>3</sup>/s) to provide water service to downstream users. The pressure head  
 95 delivered to downstream users  $H_d$  (m) is made up of the minimum pressure head required,  $H_{min}$   
 96 (m), and surplus head,  $H_{surplus}$  (m).

97 The energy components indicated in Figure 1 are defined in Table 1 and described below.

$$E_{supplied} = E_{delivered} + E_{ds} + E_{leak} + E_{friction} + E_{local} \quad (\text{Joules}) \quad (1)$$

98 where  $E_{supplied}$  = energy supplied to the upstream end of the pipe (Joules);  $E_{delivered}$  = energy  
 99 delivered to the user (in Joules) to satisfy demand  $Q_d$  (m<sup>3</sup>/s) at pressure head  $H_d$  (m);  $E_{ds}$  = energy  
 100 that flows out of the pipe to meet downstream user demands (Joules);  $E_{leak}$  = leak energy  
 101 (Joules);  $E_{local}$  = local energy losses (Joules). The term  $\alpha$  is equal to 1.85 in the Hazen-Williams  
 102 friction loss model and  $\alpha = 2$  in the Darcy-Weisbach model;  $K$  = pipe resistance and  $\Delta t$  = the  
 103 hydraulic time step (3,600 seconds or 1 hour) used in the 24-hour diurnal simulation.

## 104 **Methods**

### 105 *Metrics to Evaluate Energy Performance at the Pipe Level*

106 Five metrics have been developed to characterize the gross and net energy efficiencies,  
 107 energy needed by user, energy lost to friction, and energy lost to leakage in the pipes of a water  
 108 distribution network.

109 Gross and Net Efficiencies: The gross energy efficiency (*GEE*) in Equation 2 compares the  
 110 energy delivered to the users serviced by a pipe to the energy supplied to that pipe. The  
 111 theoretical maximum value for *GEE* is 100 percent, which means that all the energy supplied to  
 112 the pipe is delivered to its user, even though this is impossible to achieve in practice. The

113 theoretical minimum value for  $GEE$  is 0 percent, which means that none of the energy supplied  
114 to the pipe is delivered to its users, as all the energy is lost along the pipe.

$$GEE = \left( \frac{E_{\text{delivered}}}{E_{\text{supplied}}} \right) \cdot 100\% \quad (2)$$

115 The net energy efficiency ( $NEE$ ) in Equation 3 compares the energy delivered to users  
116 serviced by a pipe to the net energy in that pipe. Here, net energy is defined as the energy  
117 supplied to the pipe minus the energy supplied to users located downstream of the pipe and not  
118 directly serviced by the pipe. The maximum value of  $NEE$  is 100 percent, where all the energy  
119 supplied (exclusively to the pipe) is delivered to its users. The theoretical minimum value is 0  
120 percent, where none of the energy supplied to the pipe is delivered to its users.

$$NEE = \left( \frac{E_{\text{delivered}}}{E_{\text{supplied}} - E_{\text{ds}}} \right) \cdot 100\% \quad (3)$$

121 Energy Needed by User: The energy needed by the users ( $ENU$ ) at a node in Equation 4  
122 compares the energy delivered to the users serviced by a pipe against the minimum energy  
123 needed by those users. A value of  $ENU$  below 100 percent indicates that there is an insufficient  
124 level of energy to meet the service expectations of the users (either in the form of flow, pressure  
125 head, or both), and a value of 100 percent means that energy delivered to the users is equal to the  
126 minimum energy needed to meet their service expectations. Values of  $ENU$  above 100 percent  
127 denote a surplus energy over and above the level needed.

$$ENU = \left( \frac{E_{\text{delivered}}}{E_{\text{need}}} \right) \cdot 100\% \quad (4)$$

128 The minimum mechanical energy in the water needed to meet the minimum needs of the  
129 downstream user in Equation 4 is calculated by integrating the minimum needed power by a

130 defined period of use  $\Delta t$

$$E_{\text{need}} = \gamma Q_{\text{min}} H_{\text{min}} \Delta t \quad (\text{Joules}) \quad (5)$$

131 where  $\gamma$  = unit weight of water (approximately 9,810 N/m<sup>3</sup> at 18°C);  $Q_{\text{min}}$  = minimum water  
132 use needed by users (m<sup>3</sup>/s);  $H_{\text{min}}$  = minimum pressure head required to deliver acceptable water  
133 service to users (m);  $\Delta t$  = time step over which minimum needed power is integrated (seconds).  
134 (Note that integration can be used to calculate minimum energy needed over a continuous diurnal  
135 demand period.). Determining the minimum water use ( $Q_{\text{min}}$ ) is difficult because minimum water  
136 use varies between individual users within the same user type (Friedman et al. 2013). The  
137 minimum pressure head ( $H_{\text{min}}$ ) required is usually determined by water utility standards but in  
138 reality can vary across users depending on their subjective perception of the minimum pressure  
139 required to perform their individualized water use activities (Mays 2002, City of Toronto 2009,  
140 Region of Peel 2010, Denver Water 2012). In this paper, the minimum pressure of approximately  
141 30 metres (m) commonly imposed by North American water utilities (City of Toronto, 2009;  
142 Region of Peel, 2010; Denver Water, 2012) was used to calculate the minimum mechanical  
143 energy.

144 Energy Lost to Friction: The energy lost to friction (*ELTF*) in Equation 6 compares the  
145 magnitude of friction loss in the pipe (to satisfy the demand and leakage at the end of the pipe,  
146 and demands downstream of the pipe) to the net energy supplied to the pipe. This indicator can  
147 be used to characterize the effectiveness of pipe relining, pipe replacement, and leak repair to  
148 reduce frictional losses. The metric *ELTF* can range between 0 and 100 percent, where a value of  
149 0 percent means that there are no frictional energy losses in the pipe, and a value of 100 percent  
150 means that all the net energy supplied to the pipe is lost to friction along the pipe.

$$ELTF = \left( \frac{E_{\text{friction}}}{E_{\text{supplied}} - E_{\text{ds}}} \right) \cdot 100\% \quad (6)$$

151 Energy Lost to Leakage: The energy lost to leakage (*ELTL*) in Equation 7 compares the  
 152 magnitude of energy lost to leakage relative to the net energy supplied to the pipe. The leakage  
 153 term in the numerator includes leak energy,  $E_{\text{leak}}$ , and the frictional energy loss along the pipe  
 154 required to meet the leakage flow,  $Q_l$ , at the end of the pipe  $E_{\text{friction(leak)}}$  (see Table 1). The *ELTL*  
 155 metric can range between 0 and 100 percent, where a value of 0 percent means that there is no  
 156 energy loss due to leakage in the pipe and a value of 100 percent means that all the net energy  
 157 supplied to the pipe is lost to leakage and friction to satisfy the leak in the pipe. The *ELTL* metric  
 158 can be used to characterize the effectiveness of leakage repair and pressure management in  
 159 reducing leakage energy loss.

$$ELTL = \left( \frac{E_{\text{leak}} + E_{\text{friction(leak)}}}{E_{\text{supplied}} - E_{\text{ds}}} \right) \cdot 100\% \quad (7)$$

#### 160 *Calculation of Energy Metrics*

161 The pipe-level energy metrics presented above are evaluated by following a number of steps.  
 162 First, the EPANET2 (Rossman 2000) network solver is used to calculate the hydraulic head at  
 163 model nodes and pipe flow in model links over a diurnal period. Because the pipe flow direction  
 164 may change over a day, the hydraulic head at both ends of each pipe are compared at each time  
 165 step and the node with the higher hydraulic head is identified as the upstream node. Further, to  
 166 correctly recognize to which pipes a node is an upstream node and to which pipes a node is a  
 167 downstream node, the mechanical energy that a pipe delivers to the users at its downstream node  
 168 (multiple-link node) is proportional to its flow rate and is weighted by its flow rate into its  
 169 corresponding downstream pipes, such that

$$(E_{\text{delivered}})_{i,j} = \gamma \left( \frac{Q_i}{\sum_{k=1}^m Q_k} \right) D_j H_j \Delta t \quad (\text{joules}) \quad (8)$$

170 where  $(E_{\text{delivered}})_{i,j}$  = energy delivered by pipe  $i$  to multiple-link node  $j$  (joules);  $D_j$  = demand at  
 171 downstream multiple-link node  $j$  located downstream of pipe  $i$  ( $\text{m}^3/\text{s}$ );  $H_j$  = hydraulic head at  
 172 multiple-link node  $j$  located downstream of pipe  $i$  (m);  $Q_i$  = flow in pipe  $i$  ( $\text{m}^3/\text{s}$ );  $m$  = number of  
 173  $k = 1, 2, 3, \dots, m$  upstream pipes connected to the multiple-link node  $j$ . For example in Figure 2a,  
 174 upstream pipes P-1 and P-2 with flow rates of 1.3 litres per second (L/s) and 1.6 L/s are  
 175 connected to downstream node J-1 (multiple-link node) with a demand of 2.1 L/s. Pipes P-3 and  
 176 P-4 are located downstream of node J-1. The mechanical energy ( $\gamma D H \Delta t$ ) delivered by Pipe 1  
 177 is weighted by the ratio of its flow to the total flow conveyed by the upstream pipes, or  
 178  $1.3/(1.3+1.6)$ .

179 Once the upstream and downstream nodes of each pipe have been determined, and the energy  
 180 delivered to each node resolved as described above, the hydraulic heads and pipe flows  
 181 simulated over the diurnal period are used to calculate the energy components in Table 1 to  
 182 evaluate the pipe-level metrics in Equations 2-7. An example is shown in Equation 9 where  
 183 hourly values of  $E_{\text{delivered}}$  and  $E_{\text{supplied}}$  are aggregated together throughout the day to calculate a  
 184 single value of  $GEE$  that is representative of the entire day

$$GEE = \left[ \frac{(E_{\text{delivered}})_{t=1} + (E_{\text{delivered}})_{t=2} + \dots + (E_{\text{delivered}})_{t=24}}{(E_{\text{supplied}})_{t=1} + (E_{\text{supplied}})_{t=2} + \dots + (E_{\text{supplied}})_{t=24}} \right] \cdot 100\% \quad (9)$$

### 185 *Hydraulic Proximity Indicator*

186 In the following sections of this paper, the proximity of a pipe to a water source is considered as  
 187 a factor that can influence the energy performance of a pipe. In anticipation of this, an indicator  
 188 that characterizes the hydraulic proximity of a pipe to a nearby water source is defined in

189 Equation 10. The hydraulic proximity indicator is based on the general observation that hydraulic  
190 head or pipe flow (or both) tend to decrease as one moves away from a water source to the  
191 periphery of the system where pipes generally convey smaller flow to downstream users. The  
192 hydraulic proximity indicator is a function of the role of the pipe (transmission or distribution)  
193 and its location relative to the water source of the system or pressure zone in which it is found. It  
194 is important to note that hydraulic proximity is not an indicator of the linear distance that  
195 separates a pipe from a water source, but rather an indirect indicator of the proximity of a water  
196 main asset to a water source.

$$\text{Proximity Indicator} = Q \cdot H_s \text{ (m}^4 \text{/s)} \quad (10)$$

197 in which  $Q$  is the pipe flow (m<sup>3</sup>/s) and  $H_s$  is the hydraulic head provided at the upstream node of  
198 a pipe (m) calculated with the EPANET2.0 hydraulic model. (All heads are calculated according  
199 to a fixed datum of 0 m.) High values of the hydraulic proximity indicator as defined in Equation  
200 10 suggest that the water main is located near a water source, whereas low values suggest that  
201 the main asset is located away from a water source.

### 202 **Application of Pipe-Level Metrics to Three Distribution Systems**

203 The new pipe-level metrics were applied to a large *ensemble* of water mains across three  
204 distribution systems to examine how system operation and system improvements impinge on the  
205 spatial and temporal patterns of energy performance in drinking water mains. System #1 (Figure  
206 2b) is reported in Cabrera et al. (2010) and comprises 14 pipes (40 km), an elevated tank and a  
207 pumping station controlled by minimum and maximum tank levels. The system has a total daily  
208 demand of 79.8 ML/day with peaks at 8 am (peaking factor of 1.3) and 4 pm (peaking factor of  
209 1.3) (Figure 3). Approximately 15 percent of the total demand is lost to leakage throughout the  
210 day. The leakage is assigned to the nodes using emitter coefficients in EPANET2.0 (Cabrera et

211 al., 2010). Leakage is thus a function of time and pressure. At each time step, EPANET2 is used  
212 to calculate pressure head and leakage loss to evaluate the energy lost to leakage (*ELTL*). The  
213 average daily pressure in System #1 is approximately 35 m.

214 System #2 (Figure 4a) is a medium-sized distribution system in the US Midwest that includes  
215 1,183 pipes (166 km), 4 pumping stations and 4 elevated tanks. The water distribution system is  
216 comprised of three pressure zones to overcome an elevation difference of 99.7 m to serve a  
217 population of 20,000 people. The system has a total daily demand of 237.9 ML/day with an 8 am  
218 morning peak (peaking factor of 1.25) and a 10 pm evening peak (peaking factor of 1.67) (Figure  
219 3). The daily mean pressure is 57 m and higher than in System #1. No leakage is considered in  
220 this network.

221 System #3 (Figure 4b) is a large distribution network in the US Midwest that comprises  
222 27,231 pipes (5,500 km), 28 pumping stations, and 27 elevated tanks that serves approximately 1  
223 million customers. This system has a total daily demand of 12,765 ML/day with an 8 am  
224 morning peak (peaking factor of 1.18) and a 9 pm evening peak (peaking factor of 1.40). The  
225 system has an average nodal pressure of 53 m. Leakage is modelled as a constant demand  
226 assigned by area to model nodes based upon the results of a detailed leakage study conducted by  
227 the water utility.

## 228 **Results**

### 229 *System #1*

230 System #1 is a simple system and thus an ideal network with which to demonstrate the new  
231 pipe-level metrics by way of two management scenarios (Figure 2b). The first scenario is the  
232 Baseline (B) scenario where the pipes are unimproved. The second scenario is the Leakage  
233 Reduction (L) scenario where pipe leakage is reduced by 50 percent by reducing emitter

234 coefficients in the model. In this paper, the energy metrics are dimensionless and expressed as a  
235 percentage of i) energy supplied to the pipe ( $E_{\text{supplied}}$ ), or ii) minimum energy needed at the  
236 downstream node ( $E_{\text{need}}$ ), or iii) the net energy in the pipe ( $E_{\text{supplied}} - E_{\text{ds}}$ ). For the sake of  
237 consistency, numerical values of the metrics that range between 0 and 30 percent are considered  
238 “low”, while values that range between 30 and 70 percent are considered “moderate”, and values  
239 that range between 70 and 100 percent are considered “high”.

240 Baseline Scenario (No Improvements): The baseline results in Table 2 indicate that the  
241 presence of both frictional losses and leakage in the system produce low to moderate values of  
242  $GEE$  that range between 8 to 45 percent. This association is evident in the pipes closest to the  
243 source and that carry higher flow rates (e.g., pipes 11, 12, 111, and 113) because these pipes  
244 must convey flows destined to locations further downstream in the network. Similarly, the  
245 presence of leakage in the system produces values of  $NEE$  that range between 29 to 76 percent.

246 The results in Table 2 indicate that pipes 22 and 113 have an  $ENU$  that ranges from 110 to  
247 113 percent. These pipes are located between the tank (dominant source of water in this system)  
248 and the highest nodal demand at junction J-22, and thus the large energy surplus reflects the  
249 delivery of water to this location from the source. The pipes 31, 121, and 122 located further  
250 away from the elevated tank tend to have less surplus energy, and these pipes show an energy  
251 deficit and a numerical value of  $ENU$  that ranges between 91 to 97 percent; these pipes deliver  
252 less energy to their users due to water losses between the sources and these demand locations.

253 The baseline values of  $ELTF$  suggest that friction losses comprise 39 to 66 percent of net  
254 energy in pipes 11 and 111, both of which are in close proximity to the pumping station and  
255 carry high flows. Friction comprises 1.3 to 8.0 percent of net energy in the other pipes that  
256 convey smaller flows. Also, the results for leakage losses and  $ELTL$  suggest that pressure and not

257 leak size (as reflected in the emitter coefficient), drives the level of leakage and results in high  
258 values of *ELTL*. For example, even though pipes 113 and 123 both have a low value of emitter  
259 coefficient, their proximity to the tank in a high-pressure zone causes them to have a high  
260 leakage levels and high values of *ELTL* that range from 18.8 to 22.2 percent.

261 The results also show that *NEE* in Pipe 121, located far from the tank, is driven almost  
262 exclusively by the demand at the downstream node of this pipe (*NEE* = 55 to 61 percent from 12  
263 am to 6 am; *NEE* = 75 to 82 percent from 6 am to 6 pm), whereas the net efficiency in Pipe 11  
264 near the pump is influenced by the pumping and tank operations of the system (*NEE* = 10 to 20  
265 percent during pumping periods of 12 am to 3 am and 1 pm to 5 pm). This finding highlights  
266 how the proximity to pumps and tanks and the role of pipes in the global hydraulic performance  
267 affects the net efficiency and energy lost to friction observed in individual pipes.

268 Leakage Reduction Scenario (from 15 to 8 percent of demand): The results for the leakage  
269 reduction scenario in Table 2 indicate that reducing leakage flow from 15 to 8 percent produces a  
270 0.2 to 11.0 percent increase in the *GEE* relative to baseline because it narrows the gap between  
271 energy delivered and energy supplied. This relationship is especially true for the pipes located  
272 further downstream (e.g., pipes 121, 122, 123, 31 and 32). Similarly, all pipes see a 3.9 to 18.8  
273 percent increase in *NEE* relative to baseline as a result of leakage reduction. A reduction in  
274 leakage also increases the *ENU* (or reduces the energy deficit) by 1.7 to 10.1 percent relative to  
275 baseline because energy lost to leakage is decreased in the pipes. In most pipes, a reduction in  
276 leakage is tantamount to reduced pipe flow and therefore less energy lost to leakage and friction.  
277 For example, a reduction in leakage produces a 0.8 to 8.0 percent decrease in *ELTF* in pipes 112,  
278 113, and 121 relative to baseline. However, in smaller pipes located further downstream in the  
279 system (e.g., pipes 31, 32), the friction losses tend to increase because of an increase in pipe

280 flow—a result of reduction in leakage between the water source and these pipes. Lastly, a  
281 reduction in leakage causes a 47.2 to 57.3 percent decrease in *ELTL* in all pipes.

## 282 *System #2*

283 In System #2, the energy metrics were evaluated only for those pipes (approximately 600  
284 pipes or 60 percent of the total number of pipes) that have a non-zero downstream demand.  
285 Because leakage was not modelled for this system, only metrics *GEE*, *NEE*, *ENU*, and *ELTF*  
286 were evaluated for the baseline scenario; the impact of interventions such as leakage reduction  
287 on energy dynamics was not considered. System #2 was simulated with assumed leakage levels  
288 (no leakage, 15 percent, 30 percent) and the results (not shown) suggest that the presence of  
289 leakage produces a similar frequency distribution of the numerical values of the four energy  
290 metrics as shown in Figures 5 and 9. The absence of leakage data for System #2 does not  
291 preclude the comparison of energy dynamics in System #2 with the other two systems (Systems  
292 #1 through #3).

293 The histogram results in Figure 5 show that the *GEE* follows a bimodal distribution. Here,  
294 over 60 percent of the pipes have a low value of *GEE* that ranges from 0 to 10 percent while  
295 approximately 14 percent of the pipes have a high value of *GEE* that ranges from 90 to 100  
296 percent. It is noted that low values of *GEE* in Figure 6a do not necessarily point to a poor energy  
297 performance as these pipes tend to be located near the major system components and supply a  
298 large number of users downstream. Pipes with a high *GEE* tend to be located near dead-end  
299 zones where most of the energy supplied to the pipe is used to satisfy demand at the downstream  
300 node of the pipe. Over 90 percent of the pipes have a *NEE* that ranges from 90 to 100 percent  
301 (Figure 5). Figure 6b indicates that there are trunk mains and distribution mains near pumps and  
302 tanks with low to high values of net efficiency (0.1 to 80 percent).

303 The majority of pipes (almost 80 percent) exhibit a low *ELTF* between 0 and 10 percent  
304 (Figure 5). However a minority of pipes (almost 15 percent) had high frictional energy losses,  
305 with *ELTF* between 90 and 100 percent. These pipes are large-diameter trunk mains that carry  
306 large flows with a high average unit headloss, and are located in close proximity to a pump or  
307 tank. (In this paper, average unit headloss is calculated by taking the arithmetic average of unit  
308 headloss in a pipe over the 24-hour diurnal period.)

309 The energy performance of two representative pipes (Pipes 463 and 926 – see Figures 4a  
310 and 6) during the 24-hour diurnal period was also examined (Figure 7). Pipe 463 is a 300 mm CI  
311 water main located near pumping station P1 in System #2 and conveys flows between 15-86 L/s  
312 throughout the service day. Not surprisingly, the *ELTF* in Pipe 463 varies in lockstep with the  
313 flow in the pipe, whereby *ELTF* varies between 0.1 to 3 percent during low-demand periods  
314 and *ELTF* varies between 5 to 27 percent during high-demand periods. The net energy efficiency  
315 in Pipe 463 varies widely during the 24-hour diurnal period, with values of *NEE* between 72 and  
316 86 percent during high-demand periods and values between 92 to 100 percent during low-  
317 demand periods. By contrast, Pipe 926 is a 150 mm CI main located near the periphery of the  
318 system (Figure 4a). This pipe conveys a near-constant flow of less than 0.10 L/s. Not  
319 surprisingly, *ELTF* is correspondingly low (near 0 percent throughout the whole day in Figure 7)  
320 and the net energy efficiency of this pipe is at a near-constant level of 100 percent. The results  
321 suggest that the energy performance (in this case efficiency and friction) of a pipe is contingent  
322 on the proximity of that pipe to a pump or tank.

323 The influence of the distance between a pipe and a major component on the energy performance  
324 of that pipe was examined further. This was done by plotting *ELTF* calculated with Equation 6  
325 and the max/min hourly value of energy lost to friction (*ELTF*-max, *ELTF*-min, Equation 9)

326 observed over the 24-hour diurnal period against the hydraulic proximity indicator (Equation 10)  
327 in Figure 8 for an *ensemble* of 684 pipes. The results suggest that *ELTF* is smaller in distribution  
328 mains located further away from water sources that convey low flows and incur small losses  
329 (*ELTF*-min near 0 percent). Pipes located close to water sources tend to have a value of *ELTF*-  
330 max of 100 percent (this occurs during the peak demand period). Figure 8 shows a high variation  
331 in *ELTF*-max in pipes located far away from water sources. This variability is likely owing to  
332 differences in diameter, roughness, and service flows across the smaller water distribution mains  
333 located on the periphery.

### 334 *System #3*

335 The energy metrics were evaluated for over 21,000 pipes, which represents approximately 77  
336 percent of pipes in System #3. In general, the findings for System #3 are similar to those for  
337 System #2 in that the frequency distribution of the numerical values of metrics follows a bimodal  
338 shape (Figure 9). The bimodal nature of the results emphasizes the variability of energy  
339 performance in complex systems when compared to a simpler system like System #1. The  
340 majority of pipes exhibit a good energy performance (high net energy efficiency, small frictional  
341 losses) and a minority of outlier pipes exhibit a poor energy performance (low efficiency, high  
342 losses).

343 The histogram in Figure 9 indicates that approximately 80 percent of pipes have a value of  
344 *GEE* that ranges between 0 and 20 percent. As noted before, low values of *GEE* do not  
345 necessarily point to a poor energy performance; in these trunk pipes the majority of the energy  
346 supplied to the pipe is transferred to users well downstream of the pipe and only a small fraction  
347 of the energy is delivered to users at the end of the pipe. Figure 9 also indicates that 2 percent of  
348 pipes have a value of *GEE* that ranges between 90 and 100 percent. In these distribution mains

349 near cul-de-sac areas, most of the energy is transferred to users directly at the end of the pipe.  
350 Approximately 90 percent of pipes have a *NEE* that ranges between 9 and 100 percent (Figure 9)  
351 but a minority of pipes (4 percent) have a low to moderate net energy efficiency that ranges  
352 between 10 and 50 percent. A detailed analysis showed that no single factor accounted for the  
353 low values of net energy efficiency in these pipes.

354 More than 95 percent of pipes have an *ENU* that ranges between 100 and 120 percent (Figure  
355 9) and over 90 percent of pipes have a low *ELTF* that ranges between 0 and 10 percent. Leakage  
356 performance for this system is good with over 95 percent of pipes having a low *ELTL* that ranges  
357 between 0 and 10 percent. Despite this generally good performance, there are a small number of  
358 outlier pipes (approximately 3 percent of total) with a moderate to high *ELTF* that ranges  
359 between 40 and 100 percent. Many of these poorly performing pipes were found to be large-  
360 diameter trunk mains that convey large flows from water sources to the rest of the system. A  
361 small number of pipes (2.5 percent of total) were also found to have a moderate to high *ELTL*  
362 that ranges between 40 and 100 percent, and this is a direct result of the assigned leakage values  
363 from the water utility leakage study.

364 The diurnal variation of *NEE* and *ELTF* in select pipes of System #3 were examined (results  
365 not shown). As before, the results suggest that proximity to a water source and magnitude of pipe  
366 flow conveyed by the pipe are both factors that have a large impact on the diurnal variation of  
367 net energy efficiency and energy lost to friction. Generally, pipes located far away from water  
368 sources convey little flow (with small headloss) and have values of *NEE* near 100 percent and  
369 *ELTF* near 0 percent throughout the day. In larger trunk mains located closer to water sources  
370 with comparatively high flow rates, *NEE* and *ELTF* track closely with diurnal variations in  
371 pumped flow in these pipes, as was also observed in System #2.

372 The influence of the distance between a pipe and a major component on the energy  
373 performance of that pipe was examined in System #3. Figure 10 plots the *ELTL* and the max/min  
374 value of energy lost to leakage (*ELTL*-max and *ELTL*-min over a 24-hour period) for each pipe  
375 (y-axis) against the hydraulic proximity indicator (x-axis). The values of the energy loss metrics  
376 *ELTL*, *ELTL*-max, and *ELTL*-min are moderate (30 to 60 percent) near water sources (proximity  
377 ranges between 3,000 and 6,000 m<sup>4</sup>/s) and moderate to high (30 to 100 percent) at the periphery  
378 of the system (proximity ranges between 0 and 250 m<sup>4</sup>/s). This relationship can be explained by  
379 two factors: 1) the trunk water mains close to a water source have a low level of leakage while  
380 the smaller distribution mains near the periphery of the system have a higher level of leakage,  
381 and 2) the values of net energy supplied to the pipe ( $E_{\text{supplied}} - E_{\text{ds}}$ , denominator of *ELTL*) are  
382 large and outweigh the energy lost due to leaks ( $E_{\text{leakage}} + E_{\text{friction(leak)}}$ , numerator of *ELTL*)  
383 because of the low level of leakage at locations near water sources. There is also a high degree of  
384 variability in the values of *ELTL* and *ELTL*-max near the periphery of the system as shown in  
385 Figure 10 (proximity ranges between 0 and 250 m<sup>4</sup>/s).

### 386 *Comparison of Energy Metrics With Average Unit Headloss and Pressure Head*

387 The usual practice is to use average unit headloss to identify pipes with high frictional line  
388 losses and pressure head (or excess pressure head) to identify which pipes are delivering excess  
389 mechanical energy to customers. Here, the energy lost to friction (*ELTF*) was compared to  
390 average unit headloss to assess their effectiveness in identifying pipes with high frictional energy  
391 losses. To do this, the five pipes with the highest values of *ELTF* and the five pipes with the  
392 highest values of average unit headloss were selected from the *ensemble* of 1,183 pipes in  
393 System #2 and their corresponding annual frictional energy loss was calculated. (Annual  
394 frictional energy loss was calculated by multiplying the frictional energy loss in a pipe over the

395 24-hour diurnal period and multiplying this daily energy use by 365 days.) This was repeated for  
396 System #3 (*ensemble* of 21,156 pipes). The results in Table 3 indicate the five pipes with the  
397 highest values of *ELTF* and average unit headloss sorted in descending order of annual frictional  
398 energy loss. Table 3 indicates that in System #2, *ELTF* and average unit headloss identified the  
399 same four pipes (69, 159, 117, 41) with the highest annual frictional energy loss, and in System  
400 #3, *ELTF* and average unit headloss both identified pipe 3464 as having the highest annual  
401 frictional energy loss. It is noted that average unit headloss identified four pipes with higher  
402 annual frictional energy loss than the *ELTF*. A possible reason for this is that average unit  
403 headloss relates more directly to annual frictional energy loss than *ELTF*.

404 In Table 4, the energy needed by user (*ENU*) and energy lost to leakage (*ELTL*) were  
405 compared to pressure head to determine their effectiveness in identifying pipes that experience  
406 the highest energy losses to leakage. Similar to the above, the five pipes with the highest values  
407 of *ENU* and the highest values of pressure head were selected from the *ensemble* of pipes in  
408 System #3 and sorted in descending order of annual energy lost to leakage. (Annual energy lost  
409 to leakage was calculated by multiplying the leak energy at the downstream node of a pipe over  
410 the 24-hour diurnal period and multiplying this daily energy use by 365 days.) The results in  
411 Table 4 suggest that the pipes identified with *ENU* and *ELTL* had higher values of annual energy  
412 lost to leakage than those identified with pressure head. The metrics of gross energy efficiency  
413 (*GEE*) and net energy efficiency (*NEE*) were not compared to average unit headloss and pressure  
414 head. The interested reader can find the model data and the implementation code for the new  
415 energy metrics in the supplemental data files appended to this manuscript.

416

417 **Discussion**

418 Previous research has shown that reducing leakage flow in distribution systems produces a  
419 corresponding reduction in energy use (Colombo and Karney 2002, 2005). Cabrera et al. (2010)  
420 found that leak-free systems required less energy per cubic metre of water delivered. Not  
421 surprisingly, the observations made in System #1 of this paper corroborate these observations,  
422 whereby a 50 percent reduction in leakage flow produced a near proportional decrease in energy  
423 lost to leakage and improved gross and net efficiency and reduced energy lost to friction.  
424 Additional observations on more realistic and more complex systems are needed to verify that  
425 this near one-to-one relationship holds for most systems.

426 The analysis of Systems #2 and #3 showed that the statistical distribution of energy  
427 performance of the pipes in these two large systems is bimodal where the majority of pipes have  
428 a good energy performance (high efficiency, low energy losses) but that an important minority of  
429 outlier pipes also have a poor energy performance (low efficiency, high energy losses to friction  
430 and leakage). The research of Dziedzic and Karney (2014) showed an asymmetrical energy  
431 performance across the Toronto distribution system such that water mains immediately  
432 downstream of treatment works had higher energy dissipation rates than pipes located further  
433 away from treatment plants. The results of the current paper corroborate this previous finding. In  
434 all three systems examined, pipes near components tended to have low gross and net efficiencies  
435 and high energy losses due to friction and leakage, while pipes located far away from  
436 components had high gross and net efficiencies and low friction and leakage losses. Pipes near  
437 components that experienced surplus pressures generally met the minimum energy needed by the  
438 users ( $ENU > 100$  percent) even if their *ELTL* was generally high. However, pipes in lower-  
439 pressure regions further away from components generally fell short of meeting the minimum

440 energy needed by the users ( $ENU < 100$  percent) and showed lower energy losses to leakage.

441 The findings of this paper showed that there is also a strong diurnal variation in energy  
442 inputs and outputs at the scale of the individual pipe. For all systems examined, the diurnal  
443 variation of energy efficiency and energy lost to friction in pipes close to components tended to  
444 be influenced heavily by pumping periods and tank-draining periods when pipe flows and losses  
445 were high in these pipes. Diurnal variation of energy efficiency and energy lost to friction in  
446 pipes located far away from components tended to be more influenced by diurnal variation in  
447 demand. These pipes had a low efficiency and high frictional losses during high-demand periods  
448 and high efficiency and low frictional losses during low-demand periods. These finding support  
449 the previous research that showed wide diurnal variations in global energy efficiencies in the  
450 Toronto distribution system, where low frictional losses and high efficiencies were observed in  
451 the night time when demand was low (Dziedzic and Karney 2014).

452 The results of this study also showed that the new metrics of *ELTF*, *ENU*, and *ELTL* may be  
453 complementary indicators of energy performance in a pipe to the traditional indicators of average  
454 unit headloss and pressure head. The results showed that the average unit headloss was on the  
455 whole more successful than the *ELTF* metric in identifying pipes with the highest annual energy  
456 frictional losses. This shows that average unit headloss is still an important measure because it is  
457 directly tied to the pumping costs borne by a water utility. Nevertheless, the *ELTF* metric could  
458 be used to evaluate the contribution of frictional losses relative to energy lost to leakage and  
459 energy lost at the point of demand in pipes selected for rehabilitation with the average unit  
460 headloss variable. Arguably, this could help water utilities understand the relative importance of  
461 friction in the context of other energy losses in their system.

462 The results also suggested that the *ENU* and *ELTL* metrics are more successful than pressure

463 head in identifying the pipes that have the greatest energy losses to leakage. This is because *ENU*  
464 and *ELTL* account for both flow and pressure head at the point of leakage that drive the  
465 mechanical energy that exits the system. These results suggest that *ENU* and *ELTL* have the  
466 potential to be good indicators of energy lost to leakage in distribution systems. However, the  
467 results of System #1 suggest that it is the pipes that have both high pressure and high leakage  
468 flow which tend to have the highest energy loss to leakage. For this reason, the results of this  
469 study suggest that pressure head or leakage flow alone are not good indicators of energy lost to  
470 leakage.

471 While the location of the pipe in the system has been found to have an important influence  
472 on energy use, there are likely synergistic effects between the proximity to a water source and  
473 other factors such as pipe diameter, pipe flow, leakage level, unit headloss that work together to  
474 determine energy performance in a pipe. This paper did not examine the underlying, combined  
475 effects of these key factors on the energy performance of pipes.

476 In order for the metrics of this paper to provide an accurate picture of energy performance in  
477 water mains, a calibrated network model is needed with good pipe data (e.g., wall roughness and  
478 diameter) and good data on the magnitude and spatial distribution of leakage. It is noted that  
479 many municipalities in Canada and the US do not have good spatially-disaggregated data on  
480 leakage and pipe roughness/diameter in their typically large pressure zones. Increasingly, these  
481 municipalities are quantifying leakage levels and pipe flows by metering small well-defined  
482 DMA (district metering area) areas that are smaller in size than traditional pressure zones. DMA  
483 sectorization and flow/leak monitoring is already well-established in European countries and  
484 other parts of the world and the metrics can be applied with good accuracy in these jurisdictions.

## 485 **Conclusion**

486 Previous research has shown the usefulness of energy metrics to examine the global or system-  
487 wide energy performance of water distribution systems (Cabrera et al. 2010; Cabrera et al.  
488 2014a, 2014b; Dziedzic and Karney 2014) and the balance between inputs and outputs of energy  
489 through friction and leakage losses. The current paper offered a complementary approach in the  
490 form of novel metrics that resolve energy performance at the spatial scale of the individual water  
491 main. The results of the paper showed that average unit headloss is on the whole more successful  
492 than *ELTF* in identifying pipes with high frictional energy losses, but that the new *ENU* and  
493 *ELTL* metrics are more successful than pressure head in identifying pipes that experience the  
494 highest energy losses to leakage. These metrics have the potential to assist water utilities in  
495 understanding the energy performance of unimproved pipes alongside cost, structural and water  
496 quality concerns. While outside the scope of this paper, water utilities can potentially leverage  
497 this pipe-level energy analysis to perform life-cycle costing that compares the cost of pipe  
498 rehabilitation against the surplus energy cost (from leakage and frictional losses) incurred in a  
499 pipe when not rehabilitated (do-nothing option) to characterize the payback period of the  
500 rehabilitation intervention.

### 501 **Acknowledgements**

502 The authors wish to thank the Natural Science and Engineering Research Council for its  
503 financial support of this research. Dr. Speight received support from the Engineering and  
504 Physical Sciences Research Council under grant EP/I029346/1. The authors also thank Mr. Brett  
505 Snider from the Department of Civil Engineering, Queen's University for his helpful comments  
506 that contributed to the progress of this research.

507 **References**

508 Alvisi, S., & Franchini, M. (2006). Near-optimal rehabilitation scheduling of water  
509 distribution systems based on a multi-objective genetic algorithm. *Civil Engineering and*  
510 *Environmental Systems*, 23(3), 143-160.

511 Alvisi, S., & Franchini, M. (2009). Multiobjective optimization of rehabilitation and leakage  
512 detection scheduling in water distribution systems. *Journal of Water Resources Planning and*  
513 *Management*, 135(6), 426-439.

514 American Water Works Association (2009). *M36 Water Audit and Loss Control Programs*.  
515 American Water Works Association, Denver, Colorado, pp. 422.

516 American Water Works Association (1991). *M32 Distribution Network Analysis for Water*  
517 *Utilities*. American Water Works Association, Denver, Colorado, pp. 39.

518 Askew, L.E., and McGuirk, P.M. (2004). "Watering the suburbs: distinction, conformity and  
519 the suburban garden." *Australian Geographer*, 35(1), 17-37.

520 Boulos, P. F., Lansey, K. E., Karney, B. W. (2006). *Comprehensive Water Distribution*  
521 *Systems Analysis Handbook for Engineers and Planners*, MWHSoft Press, Pasadena, CA, USA.

522 Cabrera, E., Pardo, M.A., Cobacho, R., and Cabrera Jr., E. (2010). "Energy audit of water  
523 networks." *Journal of Water Resources Planning and Management*, 136(6), 669-667.

524 Cabrera, E., Gómez, E., Cabrera Jr, E., Soriano, J., and Espert, V. (2014a). "Energy  
525 Assessment of Pressurized Water Systems." *Journal of Water Resources Planning and*  
526 *Management*, 141(8), 04014095: 1-12.

527 Cabrera, E., Cobacho, R., and Soriano, J. (2014b). "Towards energy labeling of pressurized  
528 water networks." *Procedia Engineering*, 70, 209-217.

529 City of Toronto (2009). *Design criteria for sewers and water mains*. Engineering and

530 Construction Services, Toronto, Ontario, Canada.

531 Colombo, A.F., and Karney, B.W. (2002). “Energy cost of leaky pipes: Toward a  
532 comprehensive picture.” *Journal of Water Resources Planning and Management*, 128(6), 441-  
533 450.

534 Colombo, A.F., and Karney, B.W. (2005). “Impacts of leaks on energy consumption in  
535 pumped systems with storage.” *Journal of Water Resources Planning and Management*, 131(2),  
536 146-155.

537 Dandy, G. C., & Engelhardt, M. (2001). Optimal scheduling of water pipe replacement using  
538 genetic algorithms. *Journal of Water Resources Planning and Management*, 127(4), 214-223.

539 Denver Water (2012). Engineering Standards 14th Ed., Denver, Colorado.

540 Dziedzic, R., & Karney, B. W. (2015). Energy Metrics for Water Distribution System  
541 Assessment: Case Study of the Toronto Network. *Journal of Water Resources Planning and*  
542 *Management*, 141(11), 04015032.

543 Dziedzic, R. M., and Karney, B. W. (2014). “Water Distribution System Performance  
544 Metrics.” *Procedia Engineering*, 89, 363-369.

545 Fontana, N., Giugni, M., & Portolano, D. (2011). Losses reduction and energy production in  
546 water-distribution networks. *Journal of Water Resources Planning and Management*, 138(3),  
547 237-244.

548 Friedman, K., Heaney, J., Morales, M., and Palenchar, J. (2011). “Water Demand  
549 Management Optimization Methodology.” *Journal of American Water Works Association*,  
550 103(9), 74-84.

551 Friedman, K., Heaney, J. P., Morales, M., and Palenchar, J. E. (2013). “Predicting and  
552 managing residential potable irrigation using parcel-level databases.” *Journal of American Water*

553 Works Association, 105(2), 372–386.

554 Hashemi, S.S., Tabesh, M., and Ataee Kia, B. (2013). Scheduling and operating costs in  
555 water distribution networks. *Journal of Water Management*, 166 (8), 432–442.

556 Hoekstra, A. Y., and Chapagain, A. K. (2007). “Water footprints of nations: water use by  
557 people as a function of their consumption pattern.” *Water Resources Management*, 21(1), 35-48.

558 Kleiner, Y., & Rajani, B. (2001). Comprehensive review of structural deterioration of water  
559 mains: statistical models. *Urban water*, 3(3), 131-150.

560 Lambert, A. O., Brown, T. G., Takizawa, M., & Weimer, D. (1999). A review of  
561 performance indicators for real losses from water supply systems. *Journal of Water Supply:  
562 Research and Technology-Aqua*, 48(6), 227-237.

563 Mayer, P. and DeOreo, W. (2010). “Improving Urban Irrigation Efficiency by Using  
564 Weather-based Smart Controllers.” *Journal of American Water Works Association*, 102(2), 86-  
565 97.

566 Mays, L. (2002). *Urban Water Supply Handbook*. McGraw-Hill, New York, NY.

567 Morales, M., Heaney, J., Friedman, K., and Martin, J. (2011). “Estimating Commercial,  
568 Industrial, and Institutional Water Use on the Basis of Heated Building Area.” *Journal of  
569 American Water Works Association*, 103(6), 84-96.

570 Pelli, T., and Hitz, H. U. (2000). “Energy indicators and savings in water supply.” *Journal of  
571 American Water Works Association*, 92(6), 55-62.

572 Region of Peel (2010). *Public Works Design, Specifications and Procedures Manual*. Region  
573 of Peel, Mississauga, Ontario, Canada.

574 Roshani, E., & Filion, Y. R. (2013). Event-based approach to optimize the timing of water  
575 main rehabilitation with asset management strategies. *Journal of Water Resources Planning and*

576 *Management*, 140(6), 04014004.

577 Rossman, L.A. (2000). *EPANET2: User's Manual*. US Environmental Protection Agency.

578 Cincinnati, OH.

579 Vickers, A. (2001). *Handbook of Water Use and Conservation*. Water Flow Press. Amherst,

580 Massachusetts.

581

582 Table 1. Energy inputs and outputs linked to fluid flow in a pipe.

583 Table 2. Numerical values of metrics *GEE*, *NEE*, *ENU*, *ELTF*, and *ELTL* for the baseline and  
584 leakage reduction scenarios in System #1 (reported in Cabrera et al. (2010)). *GEE*: Gross Energy  
585 Efficiency; *NEE*: Net Energy Efficiency; *ENU*: Energy Needed by User; *ELTF*: Energy Lost to  
586 Friction; *ELTL*: Energy Lost to Leakage.

587 Table 3. Pipes with the highest values of average unit headloss and energy lost to friction (*ELTF*)  
588 in System #2 (*ensemble* of 1,183 pipes) and System #3 (*ensemble* of 21,156 pipes). (Pipes are  
589 sorted by annual frictional energy loss in descending order.)

590 Table 4. Pipes with the highest values of pressure, energy needed by user (*ENU*), and energy lost  
591 to leakage (*ELTL*) in System #3 (*ensemble* of 21,156 pipes). (Pipes are sorted by annual energy  
592 lost to leakage in descending order.)

593

594 Table 1.

595

---

<b>Energy Components</b>	<b>Equations</b>
Energy supplied	$E_{\text{supplied}} = \gamma Q H_s \Delta t$
Energy delivered	$E_{\text{delivered}} = \gamma Q_d H_d \Delta t$
Minimum energy needed to meet the end-user demand in an pipe	$E_{\text{need}} = \gamma Q_d H_{\text{min}} \Delta t$
Energy that flows out of pipe to meet downstream demands	$E_{\text{ds}} = \gamma Q_{\text{ds}} H_d \Delta t$
Leak energy	$E_{\text{leak}} = \gamma Q_l H_d \Delta t$
Energy lost to friction to meet demand	$E_{\text{friction(demand)}} = \gamma [K (Q_d)^\alpha ] Q_d \Delta t$
Energy lost to friction to meet leakage	$E_{\text{friction(leak)}} = \gamma [K (Q_l)^\alpha ] Q_l \Delta t$
Energy lost to friction (meet d/s demand)	$E_{\text{friction(ds)}} = \gamma [K (Q_{\text{ds}})^\alpha ] Q_{\text{ds}} \Delta t,$ where $Q_{\text{ds}} = Q - Q_d - Q_l$

---

596

597

598

599

600

601

602

603

604

605

606

607 Table 2.

Pipe	GEE (percent)		NEE (percent)		ENU (percent)		ELTF (percent)		ELTL (percent)	
	B	L	B	L	B	L	B	L	B	L
<b>11</b>	8	9	29	29	103	106	66	68	4	2
<b>12</b>	8	8	52	52	106	108	39	42	7	3
<b>113</b>	22	23	73	73	110	115	8	8	19	9
<b>123</b>	42	47	70	70	101	111	4	4	22	11
<b>111</b>	22	24	48	48	103	108	39	40	10	5
<b>121</b>	45	48	73	73	97	104	5	5	14	7
<b>122</b>	43	47	72	72	91	98	2	2	18	9
<b>22</b>	37	37	76	76	113	116	6	7	9	5
<b>21</b>	33	35	75	75	104	109	5	6	12	6
<b>31</b>	37	39	73	73	95	102	1	2	15	7
<b>32</b>	42	45	71	71	104	112	2	2	18	9
<b>112</b>	33	36	74	74	106	111	7	7	15	7

608 B = baseline scenario; L = leakage reduction scenario.

609

610 Table 3.  
611

Pipe ID	Average Unit Headloss (m/km) <sup>c</sup>	Annual Frictional Energy Loss (MWh) <sup>d</sup>	Pipe ID	<i>ELTF</i> (Percent) <sup>e</sup>	Annual Frictional Energy Loss (MWh) <sup>d</sup>
System #2					
69 <sup>a</sup>	470.8	2,971.6	69 <sup>a</sup>	99.9* <sup>f</sup>	2,971.5
159	277.1	963.3	159	99.9*	963.3
431	131.3	644.4	117	99.9*	178.8
117	88.9	178.8	41	99.9*	150.0
41	478.2	150.0	P-97	99.9*	59.9
System #3					
3464 <sup>b</sup>	3.9	39,552.0	3464 <sup>b</sup>	99.9* <sup>f</sup>	39,552.0
26688	2.3	28,081.6	10959	99.9*	1,313.0
9706	0.1	3,908.0	8735	99.9*	894.7
10942	0.2	1,804.4	11236	99.9*	326.0
11209	0.1	1,097.2	26528	99.9*	307.3

- 612
- 613 a. Pipes with the highest average unit headloss and energy lost to friction (*ELTF*) in the *ensemble* of 1,183  
614 pipes in System #2 were sorted by annual frictional energy loss in descending order.
- 615 b. Pipes with the highest average unit headloss and energy lost to friction (*ELTF*) in the *ensemble* of 21,156  
616 pipes in System #3 were sorted by annual frictional energy loss in descending order.
- 617 c. Average unit headloss was calculated by taking the arithmetic average of hourly values of unit headloss in a  
618 pipe over the 24-hour diurnal period.
- 619 d. Annual frictional energy loss was calculated by multiplying the frictional energy loss in a pipe over the 24-  
620 hour diurnal period and multiplying this daily energy use by 365 days.
- 621 e. Energy lost to friction (*ELTF*) was calculated by taking the arithmetic average of hourly values of *ELTF* in a  
622 pipe over the 24-hour diurnal period.
- 623 f. Numerical values of *ELTF* were truncated to the tenth of a percent in the table.

624  
625

626 Table 4.  
627

Pipe ID <sup>a</sup>	Average Pressure Head (m) <sup>b</sup>	Annual Energy Lost to Leakage (MWh) <sup>g</sup>	Pipe ID <sup>a</sup>	Metric (Percent)	Annual Energy Lost to Leakage (MWh) <sup>g</sup>
Metric: <i>ENU</i> <sup>c,d</sup>					
14509	94.3	10.5	6873	123.0	17.5
14510	91.9	10.3	3443	123.4	15.8
P1379	163.1	7.3	19728	122.4	8.3
10942	92.3	6.3	19729	122.8	7.7
26572	98.8	5.3	6882	123.1	7.5
Metric: <i>ELTL</i> <sup>e,f</sup>					
14509	133.4	10.5	9540	99.0	52.2
14510	130.0	10.3	11538	97.4	15.5
19729	124.3	7.7	5898	97.8	15.2
10942	130.5	6.3	P423	99.5	11.1
19732	125.6	6.1	5877	100.0	10.2

628 a. Pipes with the highest average pressure head in the *ensemble* of 21,156 pipes in System #3 were sorted by  
629 annual energy lost to leakage in descending order.

630 b. Average pressure head was calculated by taking the arithmetic average of hourly pressure head values in the  
631 upstream and downstream nodes of a pipe over the 24-hour diurnal period.

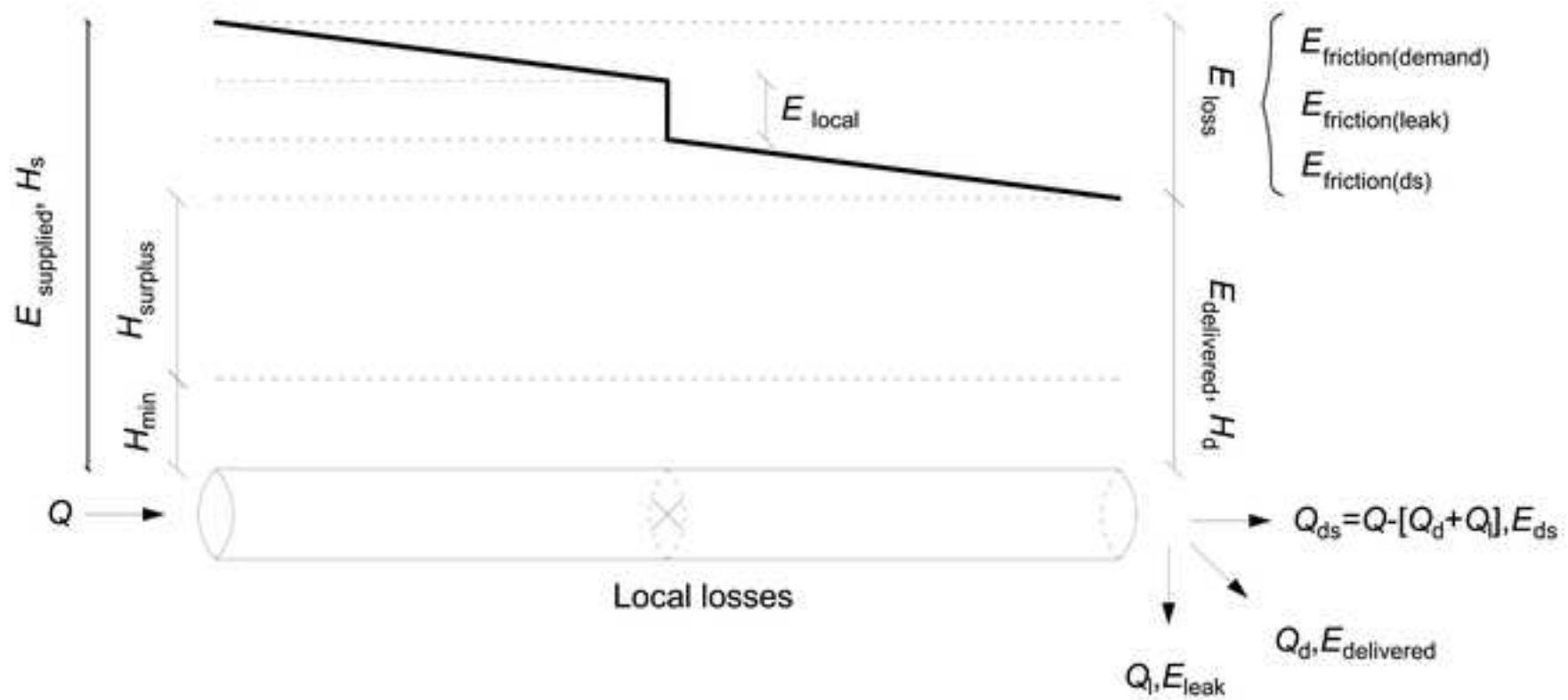
632 c. Energy needed by user (*ENU*) was calculated by taking the arithmetic average of hourly *ENU* values in a  
633 pipe over the 24-hour diurnal period.

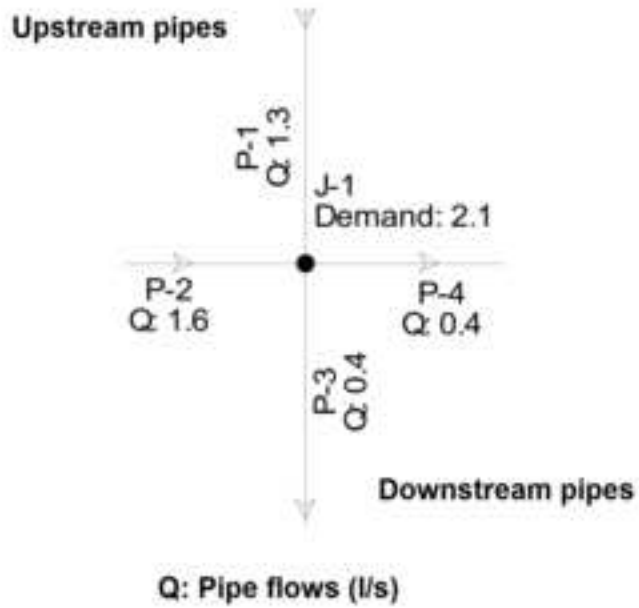
634 d. Pipes with the highest energy needed by user (*ENU*) in the *ensemble* of 21,156 pipes in System #3 were  
635 sorted by annual energy lost to leakage in descending order.

636 e. Energy lost to leakage (*ELTL*) was calculated by taking the arithmetic average of hourly *ELTL* values in a  
637 pipe over the 24-hour diurnal period.

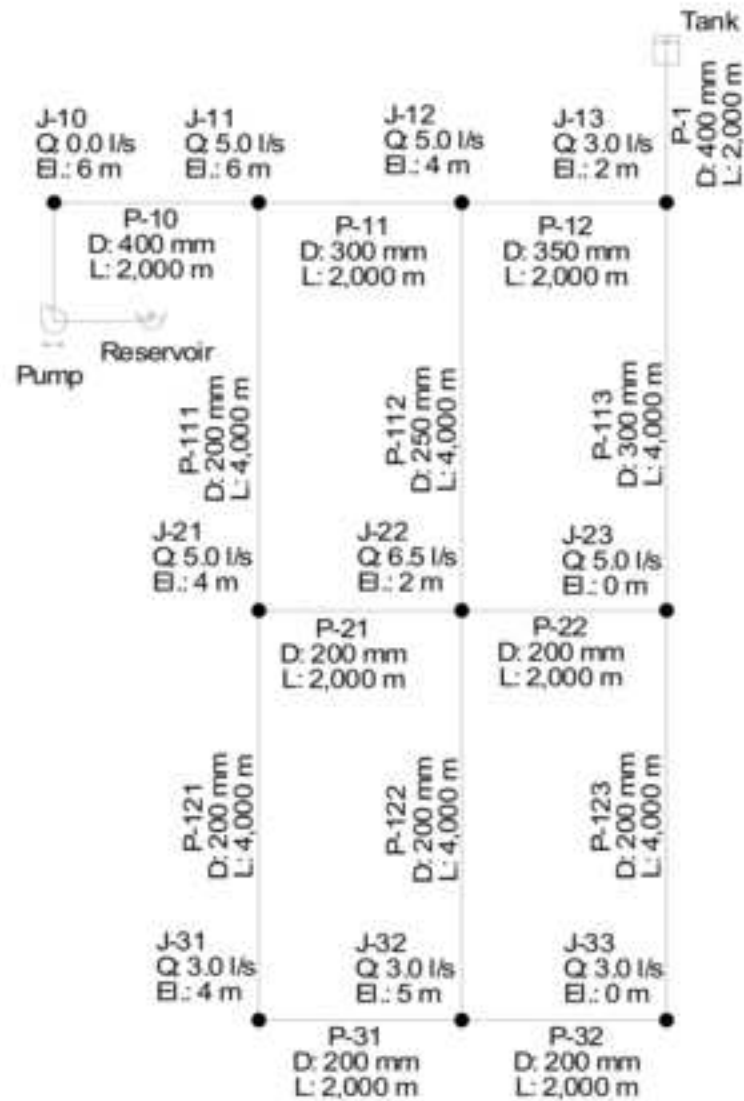
638 f. Pipes with the highest energy lost to leakage (*ELTL*) in the *ensemble* of 21,156 pipes in System #3 were  
639 sorted by annual energy lost to leakage in descending order.

640 g. Annual energy lost to leakage was calculated by multiplying the leak energy ( $E_{leak}$  indicated in Table 1) at  
641 the downstream node of a pipe over the 24-hour diurnal period and multiplying this daily energy use by 365  
642 days.





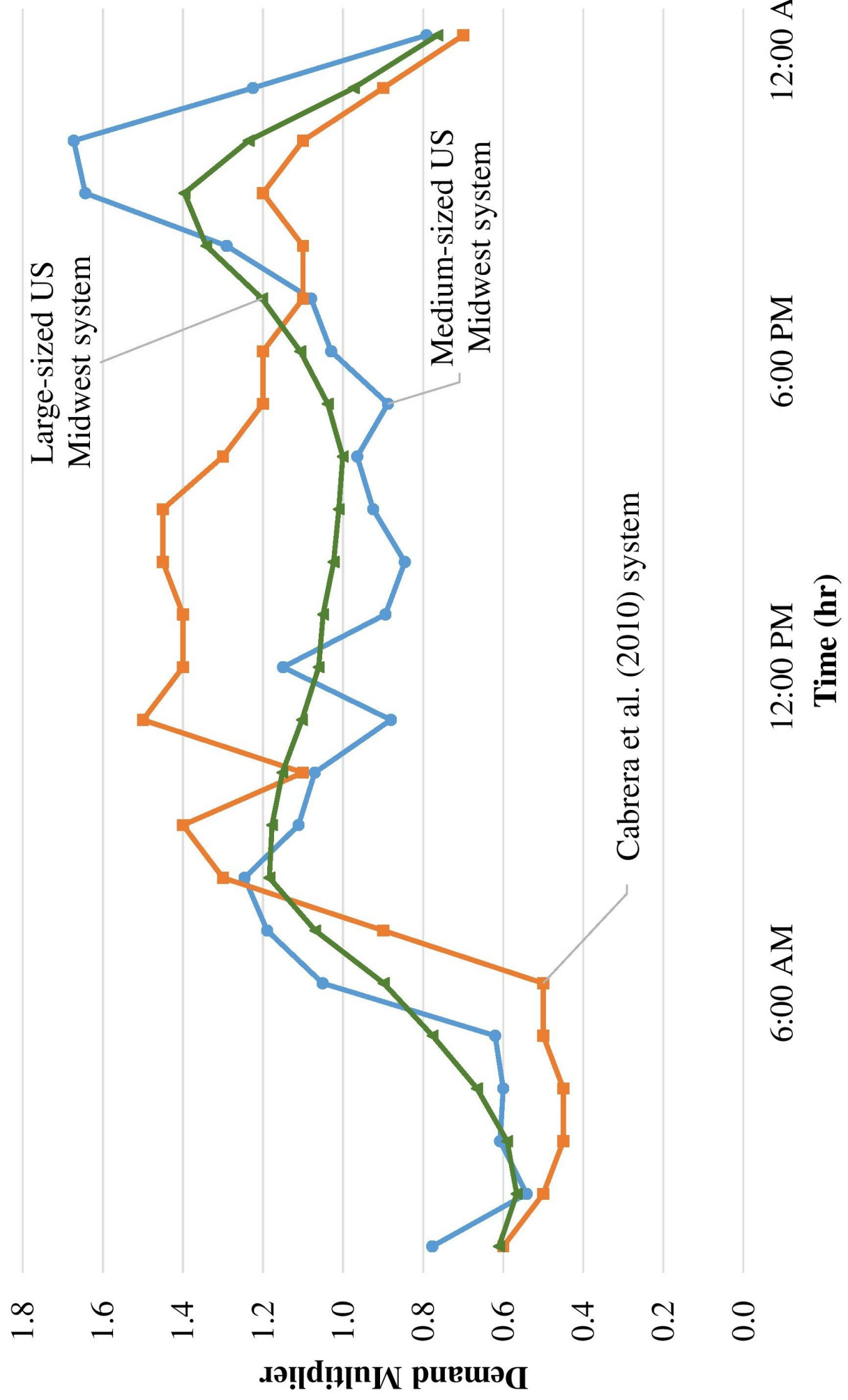
(a)



D: Pipe diameter (mm)  
L: Pipe length (m)  
El: Node elevation (m)  
Q: Nodal base demand (l/s)

(b)

Figure 3



Legend:  
—●— Medium-sized US Midwest system  
—▲— Large-sized US Midwest system  
—■— Cabrera et al. (2010) system

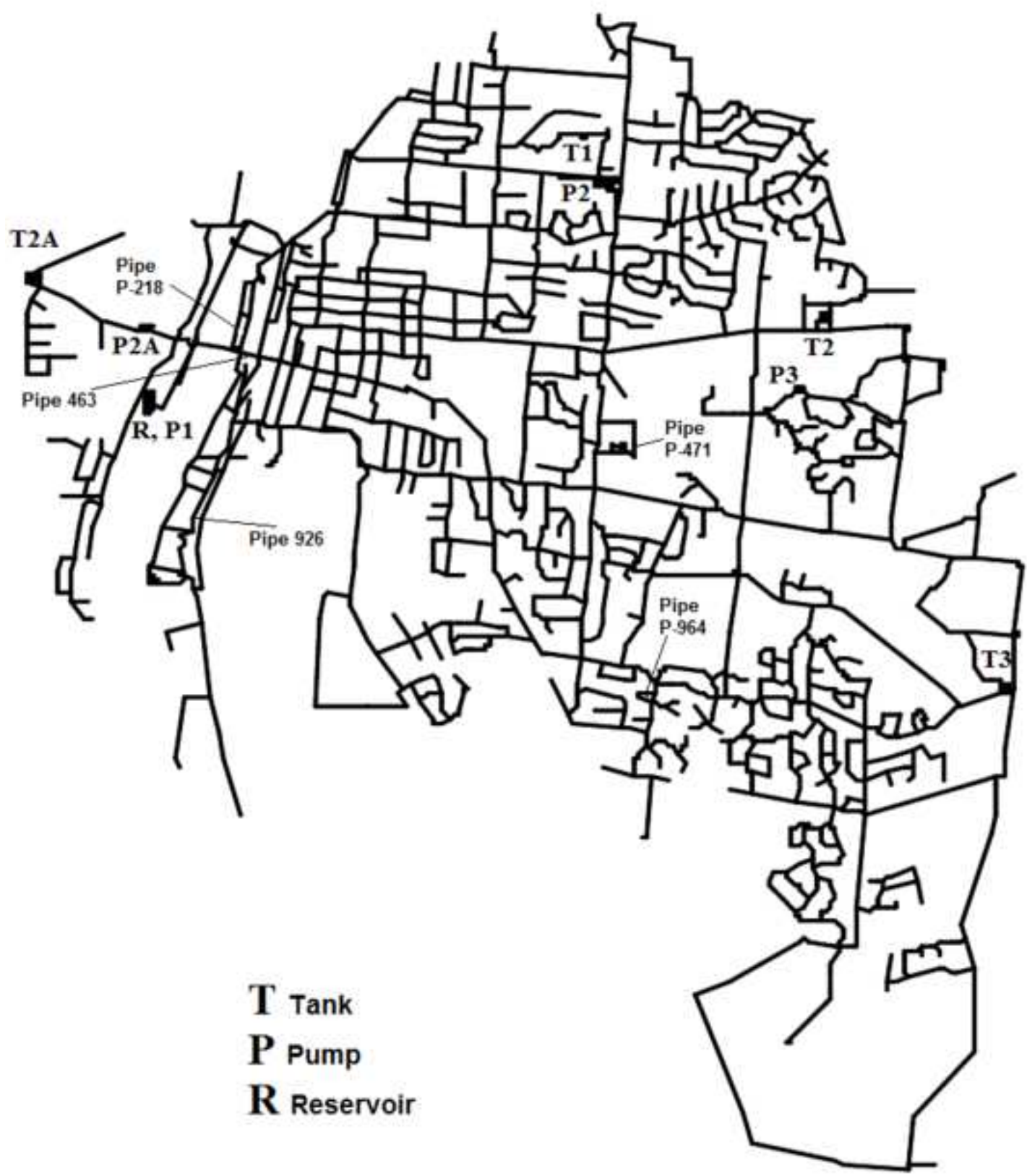
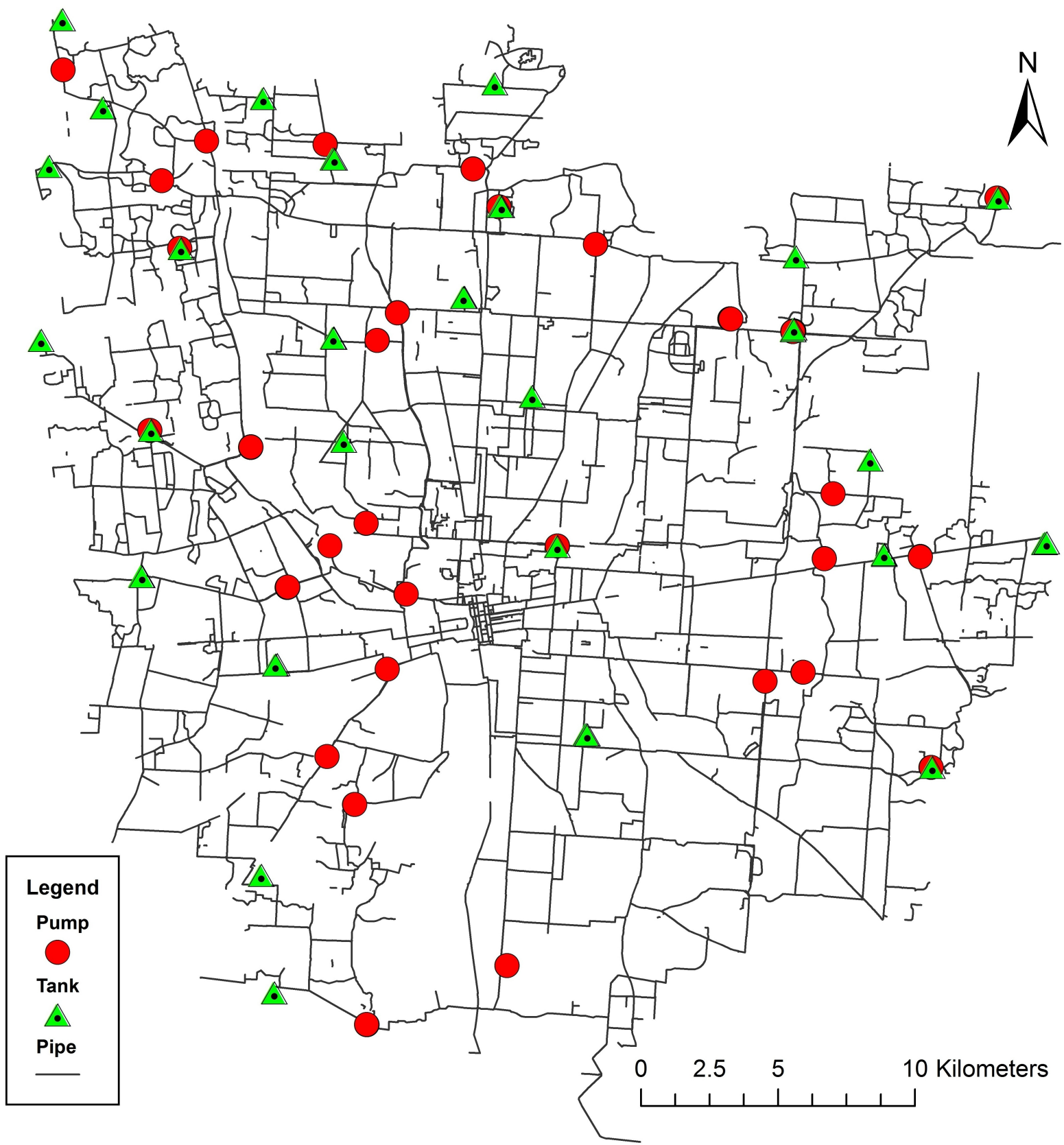
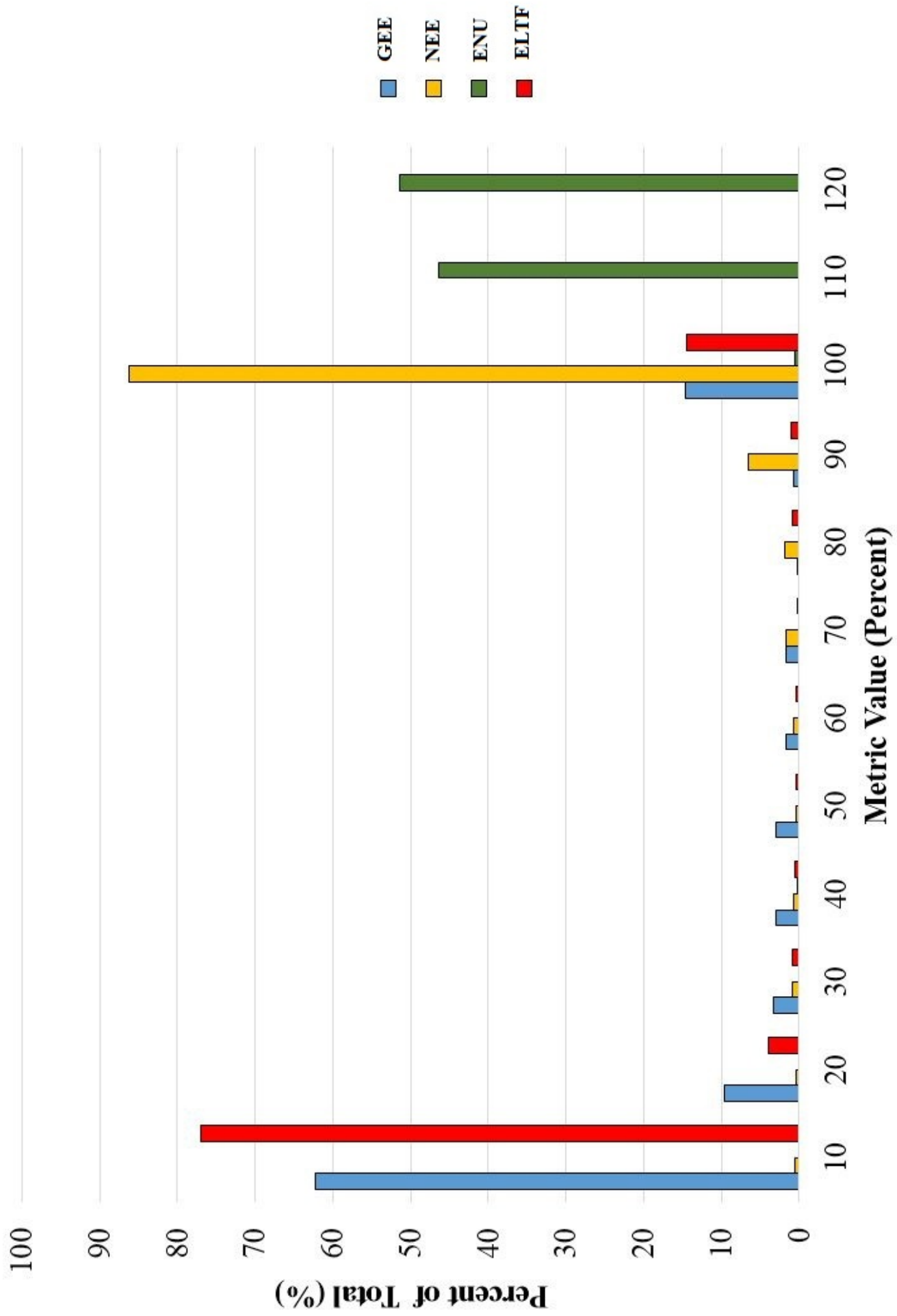
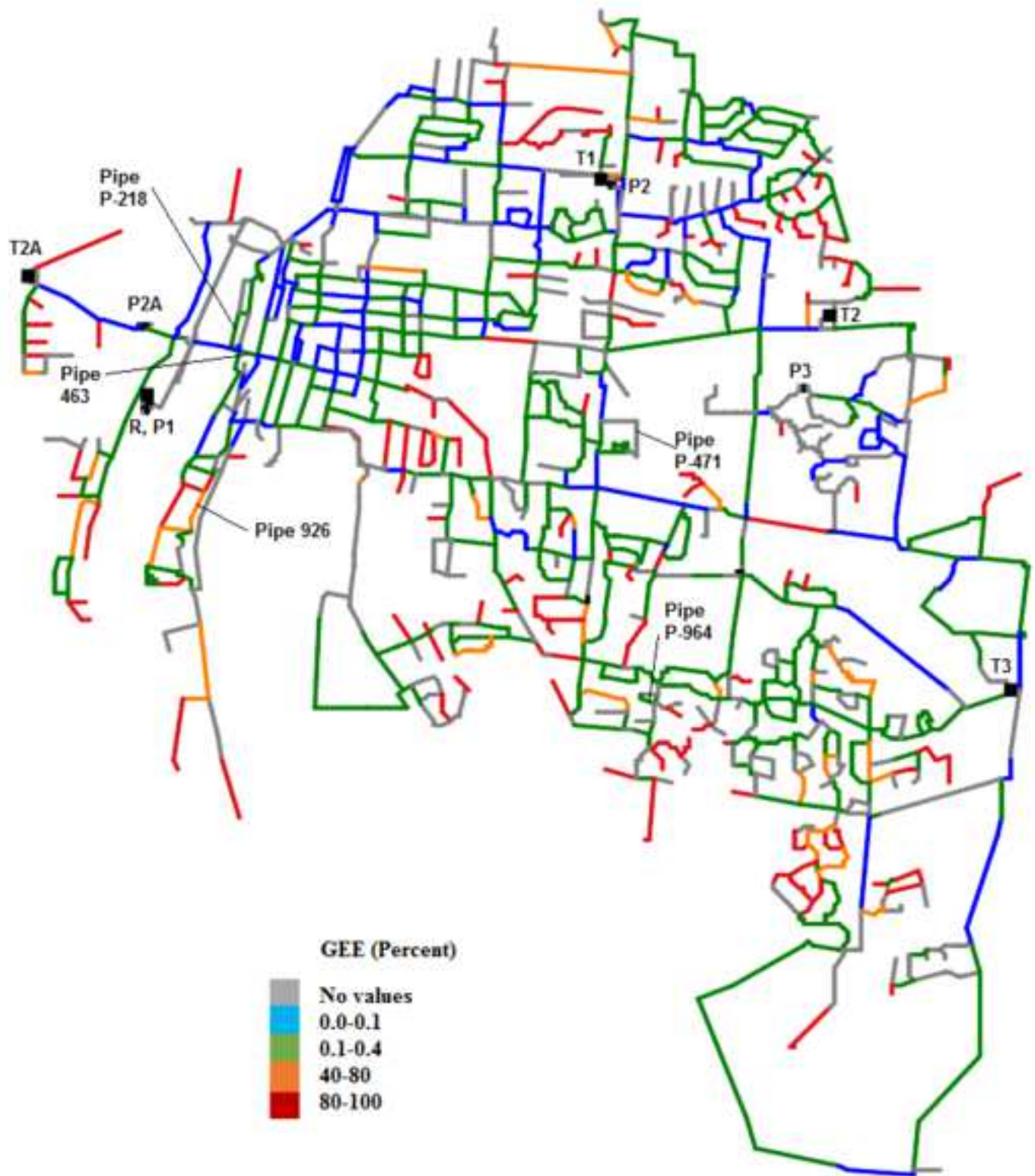


Figure 4b







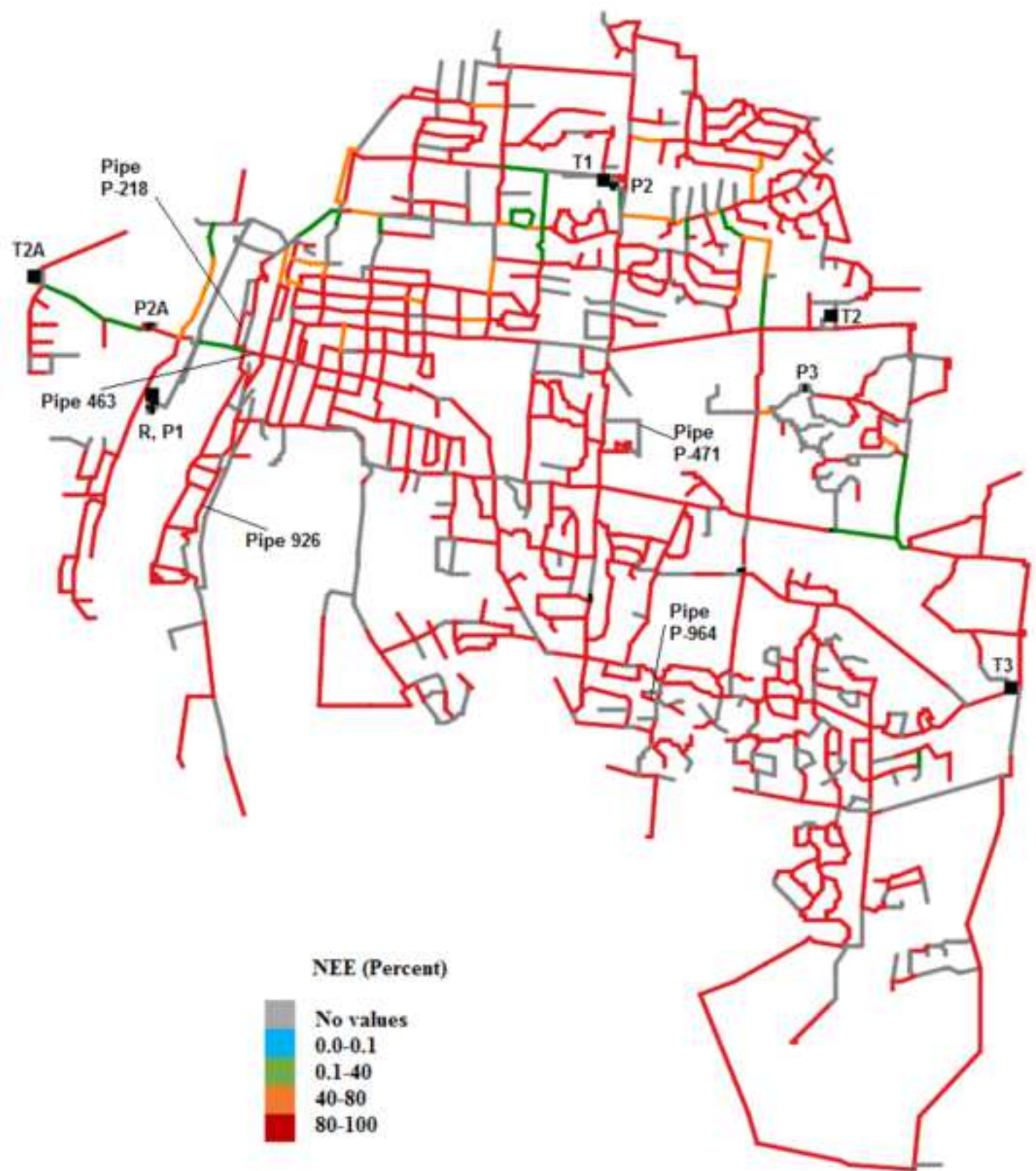


Figure 7

[Click here to download Figure Figure 7.pdf](#)

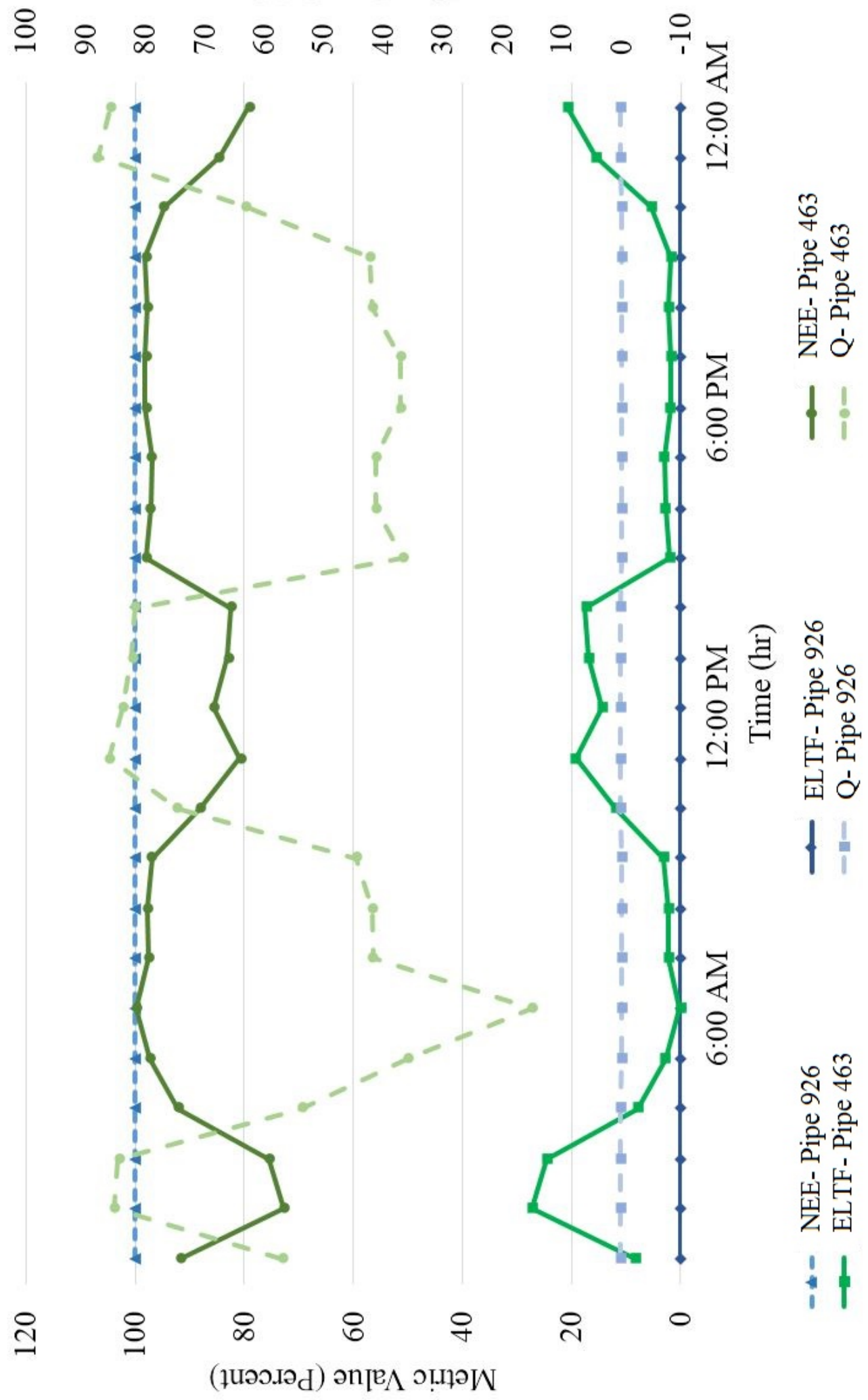
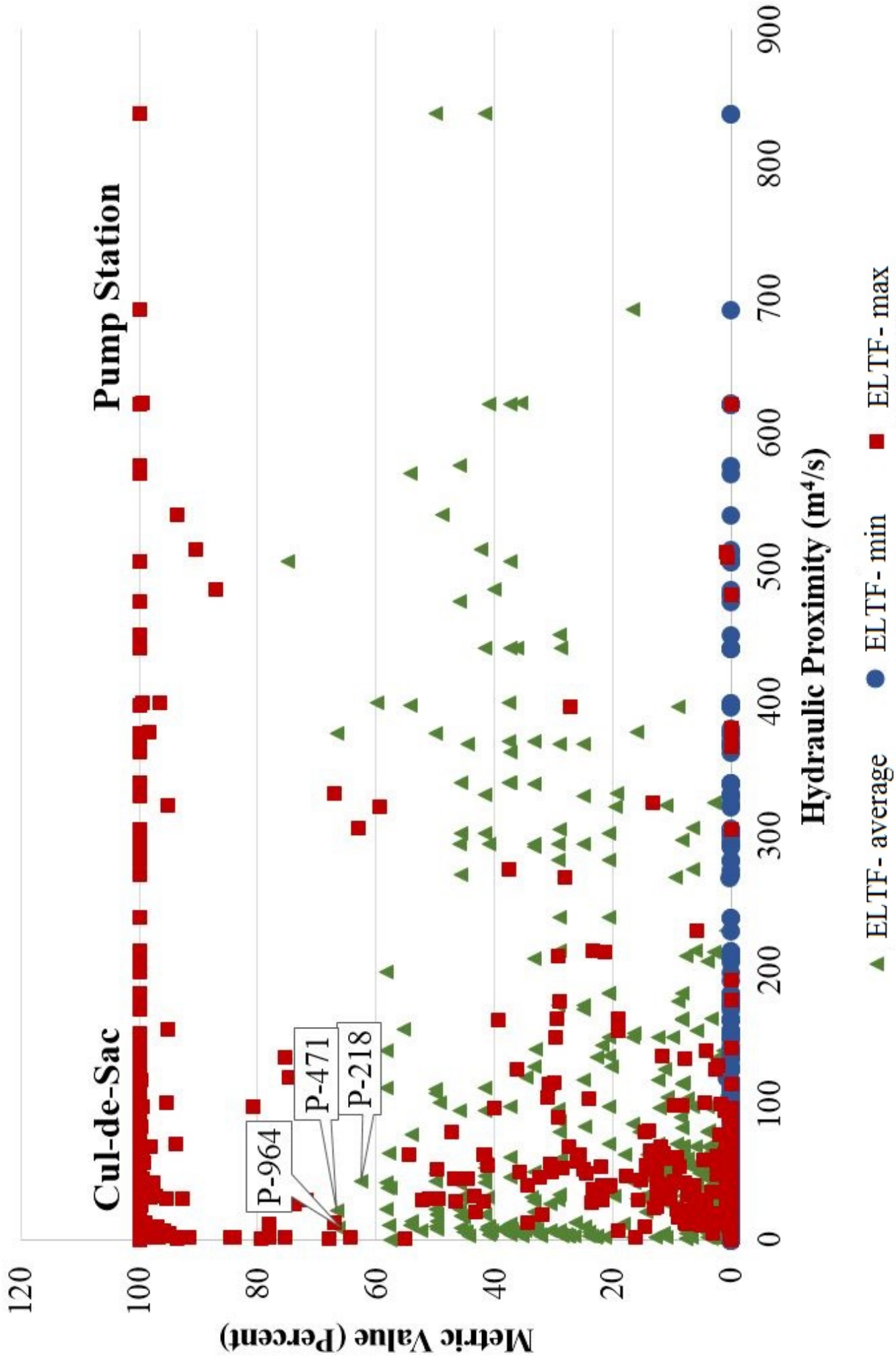
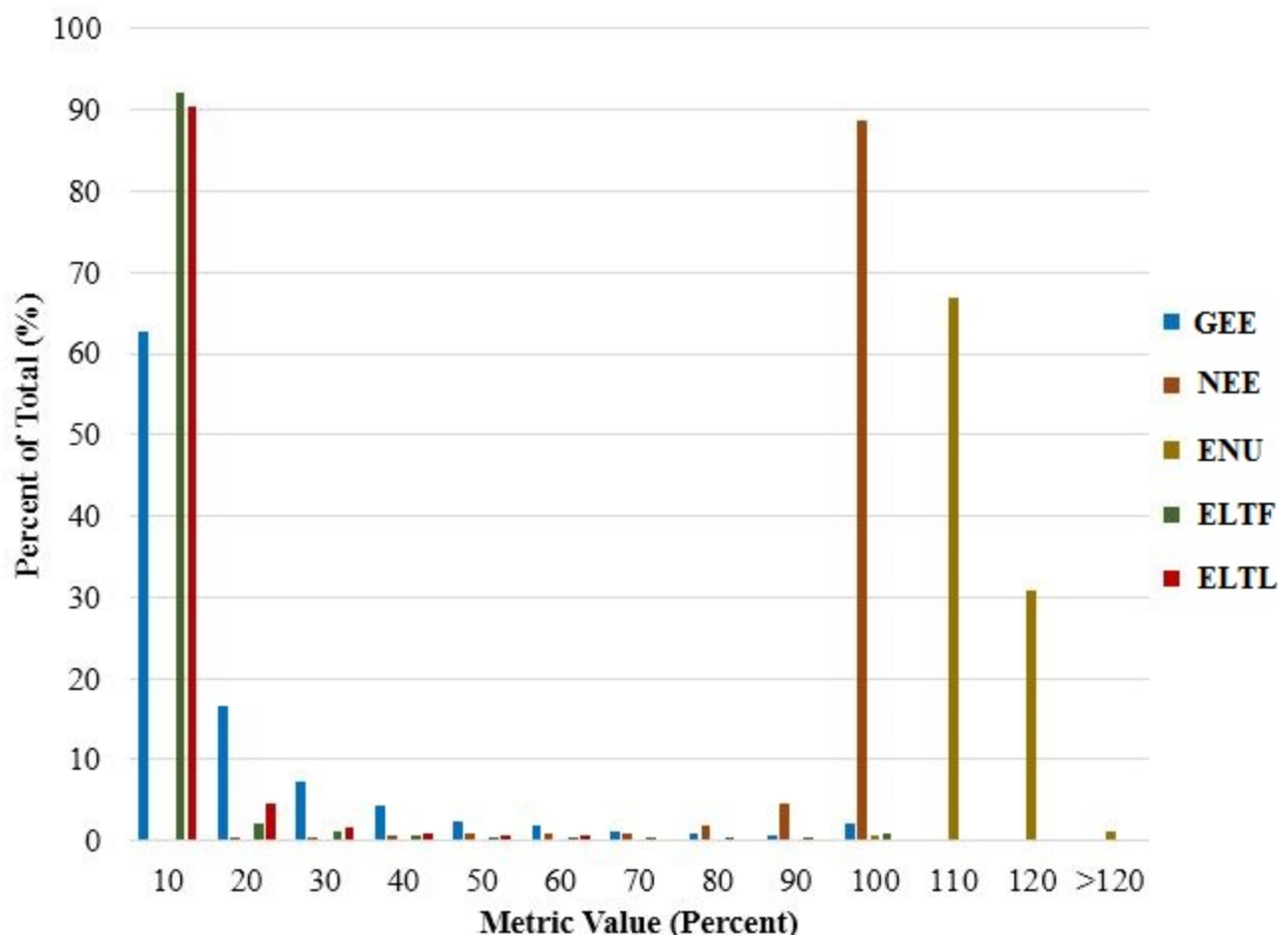


Figure 8





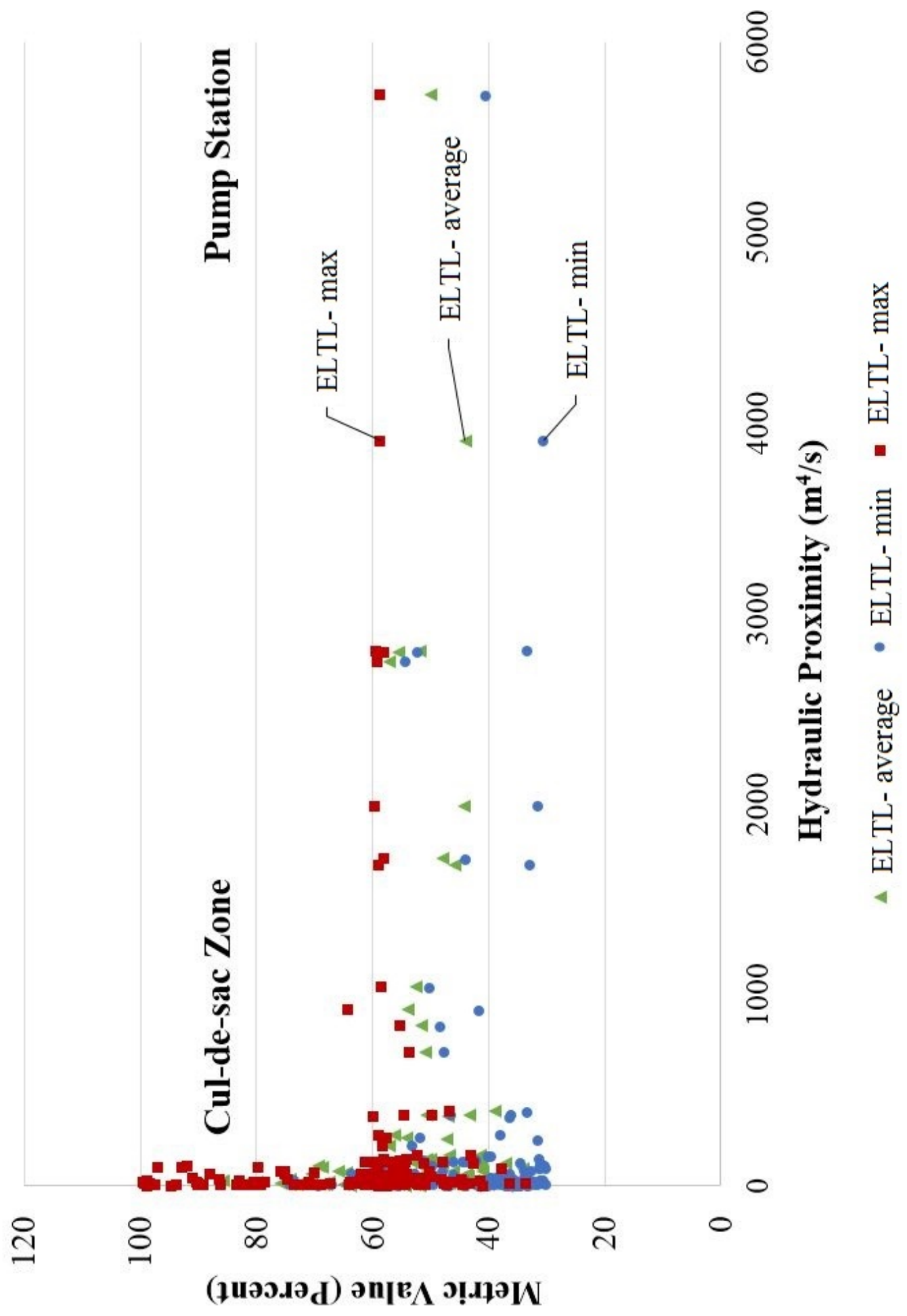


Figure 1. Hydraulic grade line and energy inputs and outputs in a pipe.

Figure 2. a) Example calculation of energy delivered at a model node connected to upstream and downstream pipes; b) model layout of System #1 (reported in Cabrera et al. (2010)) ( $L$  = pipe length;  $D$  = pipe diameter; P-10 = pipe ID; J-10 = node/junction ID;  $Q$  = pipe flow;  $El.$  = node elevation).

Figure 3. Diurnal demand pattern for Systems #1 through #3 (24-hour period).

Figure 4. a) Model layout of System #2 (medium-sized US Midwest); b) model layout of System #3 (large-sized US Midwest).

Figure 5. Histogram that indicates the percentage of pipes with numerical values of gross energy efficiency ( $GEE$ ), net energy efficiency ( $NEE$ ), energy needed by the users ( $ENU$ ) and energy lost to friction ( $ELTF$ ) in System #2 (medium-sized US Midwest) for the baseline scenario.

Figure 6. a) Numerical values of gross energy efficiency ( $GEE$ ) and (b) net energy efficiency ( $NEE$ ) in pipes of System #2 (medium-sized US Midwest) for the baseline scenario.

Figure 7. Hourly values of net energy efficiency ( $NEE$ ) and energy lost to friction ( $ELTF$ ) in Pipe 463 (near pump station P1) and Pipe 926 (located further away from pump station P1) over the 24-hour diurnal period in System #2 for the baseline scenario. (Flow in Pipes 463 and 926 are also indicated.)

Figure 8. Energy lost to friction ( $ELTF$ ) (as calculated in Eq. 6) and max/min values of energy lost to friction observed over the 24-hour diurnal period ( $ELTF$ -max,  $ELTF$ -min) versus proximity to a pump or tank component in System #2 (medium-sized US Midwest) for the baseline scenario.

Figure 9. Histogram that indicates the percentage of pipes with numerical values of gross energy efficiency ( $GEE$ ), net energy efficiency ( $NEE$ ), energy needed by users ( $ENU$ ), energy lost to friction ( $ELTF$ ), and energy lost to leakage ( $ELTL$ ) in System #3 (large-sized US Midwest) for the baseline scenario.

Figure 10. Energy lost to leakage ( $ELTL$ ) (as calculated in Eq. 7) and max/min values of energy lost to leakage observed over the 24-hour diurnal period ( $ELTL$ -max,  $ELTL$ -min) versus proximity to a pump or tank in System #3 (large-sized US Midwest) for the baseline scenario.